



Biomarkers and diatoms as tracers of past sea ice conditions and phytoplankton communities in the southwestern Ross Sea, Antarctica: drivers and variability over the last 200 years

Emma M. de Jong¹, Xavier Crosta², Sebastian Naeher^{3,a}, Bella Duncan^{1,4}, Johan Etourneau², Jae Il Lee⁵,
5 Robert McKay¹, V. Holly L. Winton^{1*}

¹Antarctic Research Centre, Victoria University of Wellington, Wellington, 6021, New Zealand

²University of Bordeaux, CNRS, Bordeaux INP, UMR 5805 EPOC, Pessac, France

³School of Geography, Environment and Earth Sciences, Victoria University of Wellington, Wellington, 6021, New Zealand

⁴Earth Sciences New Zealand, Lower Hutt, 5010, New Zealand

10 ⁵Korea Polar Research Institute, Incheon 21990, Republic of Korea

^anow at: Department of Soil and Physical Sciences, Lincoln University, Lincoln, 7647, New Zealand

Correspondence to: V. Holly L. Winton (holly.winton@vuw.ac.nz)

Abstract

15 The Ross Sea, Antarctica, is among the most seasonally productive areas globally, where different classes of phytoplankton, such as diatoms and haptophytes (*Phaeocystis antarctica*), play key roles in marine ecosystems and the carbon cycle. Sea ice dynamics strongly influence Ross Sea phytoplankton blooms, yet the effects of recent sea ice changes on bloom composition and productivity remain poorly constrained. Seasonally resolved observational records of past Ross Sea phytoplankton and sea ice variability are too short to understand potential future changes in sea ice extent, phytoplankton productivity and
20 community composition, and the resulting consequences on climate. In this study, we investigated phytoplankton-derived lipid biomarkers (fatty acids, highly branched isoprenoids; HBIs, sterols) and diatom assemblages in six marine sediment core tops and three short sediment cores collected along a north-south transect spanning two seasonally recurring polynyas in McMurdo Sound and Terra Nova Bay, to assess how sea ice dynamics and phytoplankton communities drive biomarker signatures and diatom assemblages archived in sediments. For the core-tops, we find that the proportion of open-ocean diatom species and
25 bacterial fatty acid concentrations in core top samples increases towards the southern end of the transect near McMurdo Sound, which is driven by lower summer sea ice extent, a phytoplankton community dominated by diatoms, and higher summer biomass in McMurdo Sound. In contrast, diatom assemblages shift towards sea ice-associated diatoms in the northern end of the transect, characterised by increased concentrations of sea ice diatom-derived fatty acids, sterols, and HBIs (PIPSO₂₅), driven by greater sea ice concentrations. Similarly, *Phaeocystis antarctica*-derived fatty acid biomarkers increased towards
30 the northern end of the transect, likely driven by differences in the phytoplankton community. For the short cores, we show that an exponential decrease in the fatty acid biomarker signal in the top ~20 cm of sediment is driven by processes such as bacterial biogenesis. Although phytoplankton-derived fatty acids show little change in community composition over the last 200 years, *Fragilariopsis curta* and PIPSO₂₅ indicate increasing sea ice extent, accompanied by declining *Chaetoceros* resting



spores and open ocean diatom species in the southwestern Ross Sea. Overall, our records reveal a 200-year increasing sea ice trend, consistent with existing regional sea ice extent reconstructions from ice cores. Overall, biomarkers in the southwestern Ross Sea sediment independently distinguish between pelagic diatoms, *P. antarctica*, and sea ice-associated diatoms, offering a valuable tool for developing decadal resolution records of sea ice and phytoplankton community changes.

1 Introduction

Antarctic phytoplankton form the base of the Southern Ocean marine food web and influence the rate of oceanic carbon drawdown. The Ross Sea is one of the most productive regions of the global ocean, with phytoplankton production driving the uptake and storage of carbon dioxide (CO₂) in the ocean, decreasing local atmospheric CO₂ compared to the global average (Arrigo, 2003; Arrigo & van Dijken, 2004; Bolinesi et al., 2020; Dong et al., 2024; Henley et al., 2020; Ryan-Keogh et al., 2017; Willis et al., 2023). High primary productivity is observed across the Ross Sea, especially in three seasonal biological hotspots, Terra Nova Bay, McMurdo Sound, and the central Ross Sea, where different phytoplankton classes dominate (Arrigo et al., 2015). Antarctic phytoplankton inhabit various habitats, including within sea ice, under sea ice, or on the ice edge, as well as in the mixed layer where the bulk of primary production occurs (Pinkerton et al., 2021; Schofield et al., 2024). Diatoms represent the bulk of biomass across the Ross Sea, with notably high proportions in the Terra Nova Bay biological hotspot (Arrigo et al., 2000; Arrigo et al., 2015; Bolinesi et al., 2020; Eikrem et al., 2016; Mangoni et al., 2017). This region supports large diatom blooms due to strong water column stratification, which favours their growth (Arrigo & van Dijken, 2004). In contrast, the central Ross Sea typically features a deeper mixed layer, and haptophytes, most notably *P. antarctica*, are present in similar abundances with diatoms, as they can thrive without upper ocean stabilisation (Arrigo et al., 2000; Arrigo et al., 2015; Bolinesi et al., 2020; Eikrem et al., 2016; Mangoni et al., 2017). Despite these general patterns, interannual variability is observed. For example, *P. antarctica* blooms can dominate in Terra Nova Bay, contributing to almost 80% of the total cell counts (Mangoni et al., 2019). Similarly, phytoplankton blooms in McMurdo Sound appear to fluctuate between diatom (Arrigo et al., 2000; Hayward et al., 2023; Hayward et al., 2025; McMinn et al., 2010) and *P. antarctica* blooms (Mangoni et al., 2017; Stoecker et al., 1995). The proportion of different phytoplankton classes can have widespread ecological and climatic impacts. *Phaeocystis antarctica*, for instance, can form large colonies, which may lead to lower grazing rates relative to diatom blooms and more carbon export to the ocean floor (Arrigo et al., 2000; Elliott et al., 2009; Mangoni et al., 2019; Mangoni et al., 2017; Saggiomo et al., 2021).

Seasonal phytoplankton blooms in the Ross Sea are driven by sea ice conditions, water stratification, temperature, direct light availability, and the availability of iron, a bio-limiting nutrient for phytoplankton growth and macronutrients (Arrigo et al., 2015; Hayward et al., 2025; Winton et al., 2016). Variability in sea ice drives complex changes in the timing, duration, magnitude and composition of phytoplankton and sea ice algae blooms by creating different open-ocean and under-ice habitats for phytoplankton to inhabit (Cau et al., 2021; Mangoni et al., 2017; Pinkerton et al., 2021; Schofield et al., 2024). Climate change is predicted to impact the Southern Ocean biogeochemistry via light availability, micronutrient abundance, ocean



acidification, salinity, sea ice extent, and water temperature changes, which will affect the structure, function, and abundance of phytoplankton in the Southern Ocean (Boyd et al., 2015; Deppeler & Davidson, 2017; Henley et al., 2020; Willis et al., 2023). However, our understanding of sea ice and phytoplankton relationships in the Ross Sea currently relies on only a couple of decades of continuous satellite-derived chlorophyll *a* data (Deppeler & Davidson, 2017). Longer baseline records are required to understand the natural variability of sea ice and accurately predict changes to sea ice extent as well as impacts on phytoplankton community composition and abundance. Sediment cores offer an opportunity to investigate past sea ice and phytoplankton changes on longer timescales. Past reconstructions of sea ice and phytoplankton changes have typically been determined using biogenic silica, total organic carbon and microfossil/diatom abundances (Cunningham et al., 1999; Leventer et al., 1993; Mezgec et al., 2017; Thomas et al., 2019). In the Ross Sea, only a few records document sea ice changes over the last 200 years, an important period to contextualise recent change (Thomas et al., 2019). Diatom studies in McMurdo Sound and Granite Harbour report increases in sea ice over the last 500-1000 years and a decrease in diatoms associated with high productivity (Leventer & Dunbar, 1988; Leventer et al., 1993). In addition, biogenic silica and microfossil analyses only record siliceous material, leaving other classes of phytoplankton, such as haptophytes and more specifically *P. antarctica*, unrepresented in paleorecords due to the lack of fossils produced by these species. Reconstructions of *P. antarctica* abundances through time are valuable to understand past and future community dynamics and carbon cycling (Arrigo et al., 2000; Elliott et al., 2009; Mangoni et al., 2019; Mangoni et al., 2017; Saggiomo et al., 2021).

Biomarkers, namely highly branched isoprenoids (HBIs), fatty acids, and sterols, found in Antarctic sediments provide a more complete and specific record of past sea ice extent and phytoplankton response. IPSO₂₅ (Ice Proxy Southern Ocean), a di-unsaturated C₂₅ HBI alkene also known as ‘diene’ is suggested to be solely sourced from the diatom *Berkeleya adeliensis*, has been identified in Antarctic marine sediments and used as a sea ice algae proxy (Belt, 2018; Belt et al., 2016; Etourneau et al., 2013; Johns et al., 1999; Johnson et al., 2021; Lamping et al., 2020; Lamping et al., 2021; Sadatzki et al., 2023; Schmidt et al., 2018; Tesi et al., 2020; Vorrath et al., 2023; Vorrath et al., 2020). Fatty acids and sterols can distinguish between different phytoplankton sources, with specific compounds diagnostic of diatoms, dinoflagellates, haptophytes, and bacteria (Hamm et al., 2001; Kaneda, 1991; Nichols et al., 1993; Nichols et al., 1986; Skerratt et al., 1995; Skerratt et al., 1998; Smik, Belt, et al., 2016). In this study, we focus on the assemblage of fatty acids and two key sterols, dinosterol and brassicasterol (Vorrath et al., 2019), as well as bacterial markers (branched fatty acids), as bacteria can degrade biomarkers in Antarctic sediments.

In the Ross Sea, IPSO₂₅ has been identified in surface sediments (Belt et al., 2016) and a sediment core record reconstructing past sea ice over the last 2600 years in a localised inlet (Tesi et al., 2020). However, the Ross Sea covers a large spatial area, and records may not represent sea ice trends in the wider Ross Sea due to localised ecological and sedimentation processes. Phytoplankton biomarkers have been identified in other Antarctic regions to investigate paleo-productivity (Ashley et al., 2021). However, the restricted number of studies linking phytoplankton species sources to paleo-biomarker records in the Ross Sea and wider Southern Ocean limits our understanding of how these biomarkers relate to past sea ice and phytoplankton conditions.



Here we investigate the drivers of fatty acid and highly branched isoprenoid (HBIs) biomarkers, supported by diatom assemblages, in six shallow sediment cores along a transect of seasonally variable sea ice conditions in the southwestern Ross and discuss trends in sea ice conditions over the last 200 years.

2 Methods

2.1 Sediment samples and age model

Six individual sediment cores were collected along a north-south transect from McMurdo Sound coastal polynya to Terra Nova Bay coastal polynya in the southwestern Ross Sea in February 2014 and 2015 by the Korean Polar Research Institute vessel *RV Araon* during cruises ANA04C and ANA05B (Figure 1, Table 1). The three box cores (BC02, BC03, BC04) and the gravity cores (GC72, GC78, GC80) were mainly composed of olive grey diatomaceous mud. Crude lamination is observed at 42-45 cm in BC03 and at 0-5 cm in BC04. Twenty-seven sediment samples were subsampled from these cores at various depth resolutions (see Table 1). The first subsamples in the cores are sampled from either 0-1 cm depth or 1-2 cm depth; these samples are referred to as ‘core top’ throughout this study.

Table 1: Sample details for Ross Sea sediment samples, including sediment core name, depth of sample (cm), drill location coordinates, year collected, water depth, core length, age and age error. CFCS: constant sedimentation rate lead dating model.

Core name	Depth (cm)	Location	Year Collected	Water depth (m)	Core length (cm)	Age (years CE, CFCS model)
RS14-BC02	1-2	76°50.695'S, 163°50.611'E	2014	720	37	2007 ± 1.5
	5-6					1990 ± 5.7
	11-12					1963 ± 11.9
	15-16					1945 ± 16.0
	21-22					1919 ± 22.2
	25-26					1901 ± 26.3
	31-32					1874 ± 32
	35-36					1856 ± 37
RS14-BC03	1-2	76°05.000'S, 163°13.000'E	2014	970	47	2008 ± 0.2
	7-8					1985 ± 0.9
	13-14					1961 ± 1.7
	19-20					1938 ± 2.4
	25-26					1914 ± 3.1
	31-32					1890 ± 3.9
	37-38					1867 ± 4.6



	43-44					1843 ± 5.3
RS14-BC04	1-2	75°56.8792'S, 163°00.0206'E	2014	930	56	2007 ± 0.6
	7-8					1981 ± 3.2
	15-16					1945 ± 6.7
	21-22					1919 ± 9.2
	29-30					1883 ± 12.7
	35-36					1856 ± 15.3
	43-44					1821 ± 18.7
	49-50					1794 ± 21.3
RS15-GC72	0-1	77°14.7225'S, 164°33.7824'E	2015	944	363	
RS15-GC78	0-1	76°15.3160'S, 163°28.5318'E	2015	821	393	
RS15-GC80	0-1	76°48.2001'S, 163°55.6482'E	2015	721	444	

115 Age models were derived using ^{210}Pb dating. ^{210}Pb is quantified by determining its daughter ^{210}Po excess and excess error (Bruehl & Sabatier, 2020). Sediment samples from cores BC02, BC03, and BC04 were analysed at the Institute of Environmental Science and Research Limited (ESR) for ^{210}Po using alpha spectrometry (Appleby, 2001). Sedimentation rates and sediment ages were calculated following Appleby (2001). Briefly, the sedimentation rate was calculated from the least-squares fit slope of a plot of $^{210}\text{Po}_{\text{Supported}}$ on a logarithmic scale against depth and the constant flux and constant sedimentation rate (CFCS) model was applied due to unknown sediment density of the samples. Errors were estimated by Monte Carlo simulations using the R package 'serac' (Bruehl & Sabatier, 2020). The CFCS model produced best age estimates between 1857-2007, with an error of ± 37 years at the base for BC02 (Table 1, Supplementary Figure 1). Each sampled cm of sediment represents ~ 4 years and was sampled every 18-37 years. Best age estimates for BC03 were 1843-2008 ± 5 years at the base, and ~ 3.6 years are represented by each 1 cm sample. Sampling resolution was 24 years between each sample. BC04 was dated to 1794-2007 ± 21 years at the base, with 1 cm of sediment representing ~ 3.3 years, and was sampled every 27-36 years.

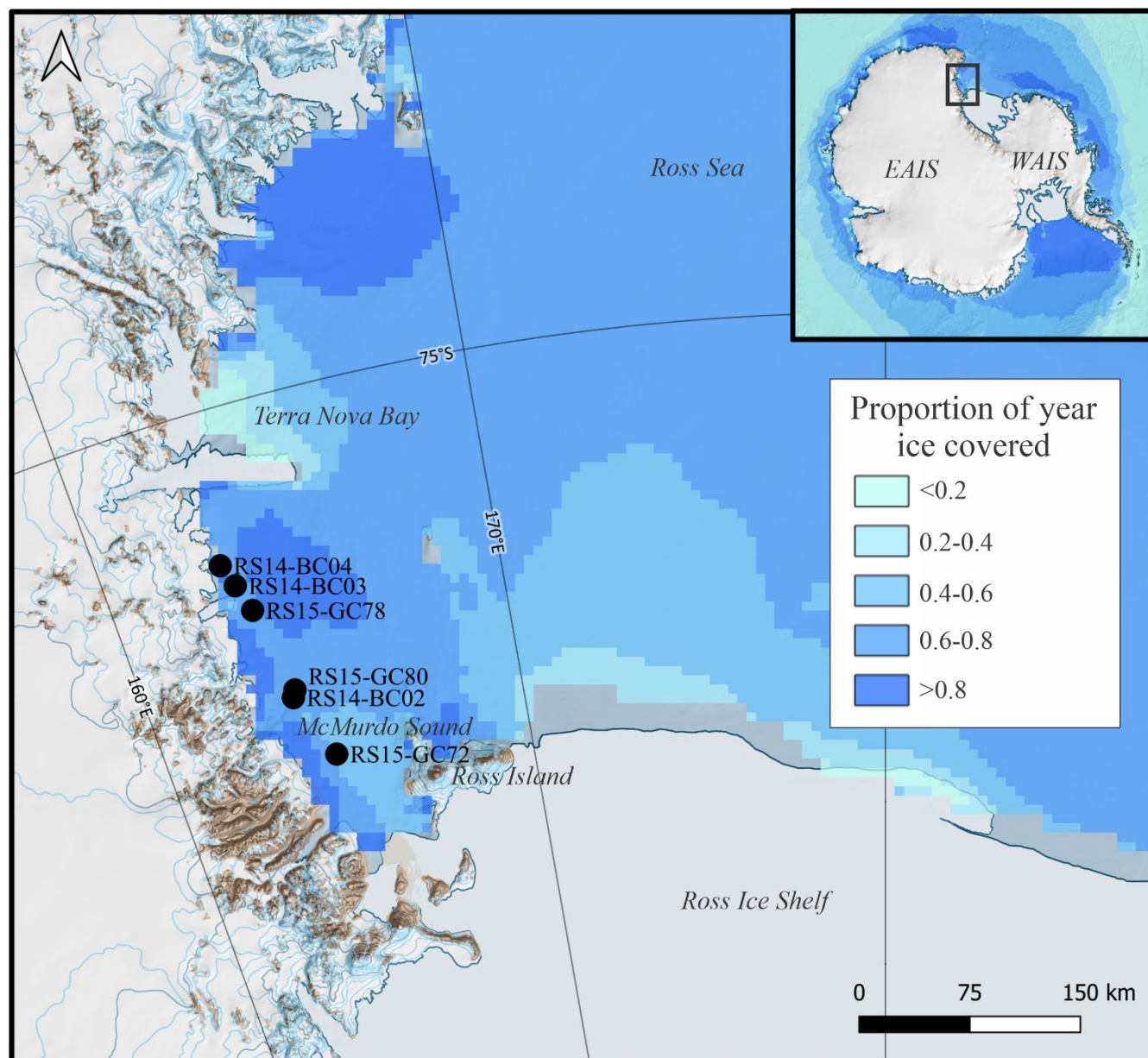


Figure 1: Location of sediment core sites (black circles) in the southwestern Ross Sea in relation to sea ice cover (average proportion of year ice covered between 2002 and 2011). Top right: Map of Antarctica, where EAIS: East Antarctic Ice Sheet, WAIS: West Antarctic Ice Sheet. Insert: Southwestern Ross Sea. Base map Quantarctica GIS package, Norwegian Polar Institute (Matsuoka et al., 2021). Average proportion of year ice covered, 6.25 km resolution (2002-2011) data source: Spreen et al. (2008).

2.2 Bulk sediment analyses

Approximately 10-15 mg of dried, homogenised, and inorganic carbon-removed sample was analysed for total organic carbon (TOC) and nitrogen (TON) via dynamic flash combustion (The FlashSmart Elemental Analyzer Thermo Fisher Scientific).



CO₂ and N₂ gases are detected by a Thermal Conductivity Detector, and the results are calibrated against three certified standards, resulting in an error of 5% for carbon and 8% for nitrogen, based on replicate measurements of soil certified standards.

2.3 Lipid biomarker analysis

Organic geochemical extraction and analysis were performed in the joint Earth Sciences New Zealand/Te Herenga Waka-Victoria University of Wellington Organic Geochemistry Laboratory following Naeher et al. (2012). Briefly, approximately 7 g of freeze-dried and homogenised sediment was extracted by ultrasonication using dichloromethane(DCM)/methanol(MeOH)(3:1, v:v). An internal standard containing 5 α -cholestane, *n*-C₁₉ alcohol, and *n*-C_{19:0} fatty acid was added to the total lipid extract (TLE) to calculate relative concentrations. The TLE was saponified with 6% KOH in MeOH and the fatty acids were separated from the neutral compounds and derivatised by boron trifluoride in MeOH to fatty acid methyl esters (FAMES). To determine the number and position of double bonds, the FAME fractions were derivatised with 2-amino-2-methyl-1-propanol (AMP) to form 2-alkenyl-4, 4-dimethoxyloxazline (DMOX) derivatives. The neutral compounds were separated into three fractions by silica gel column chromatography using *n*-hexane, *n*-hexane:DCM (1:2), and DCM:MeOH (1:1) to obtain apolar fraction containing HBIs (F1), the ketone fraction (F2), and the polar fraction (F3). The F3 fraction was derivatised prior to analysis using pyridine and N, O-Bis(trimethylsilyl)trifluoroacetamide. Procedural blanks were used for data quality control and to investigate any potential laboratory contamination.

2.4 Gas chromatography-mass spectrometry

Samples were analysed on a gas chromatography mass spectrometer (GC-MS; Agilent Technologies, model: 7890A and 5975C) with a 60-metre-long capillary column (Agilent J&W DB-5MS, inner diameter of 250 μ m, and film thickness of 0.25 μ m), and helium as the carrier gas (1 mL min⁻¹). Fatty acids and apolar fractions were injected on the GC-MS splitless at an inlet temperature of 300°C, and the MS was operated in full scan (*m/z* 50–700). The temperature program of the oven was 70°C, 70–150°C at 20°C min⁻¹, 150–320°C at 4°C min⁻¹ and then kept isothermal at 320°C for 15 minutes. The derivatised polar fraction and DMOX fatty acid derivatives were injected and analysed as above, except the GC-MS was kept isothermal at 320°C for up to 25 minutes.

2.5 Data processing and interpretation

Lipids were identified by retention time, total ion current (TIC) mass spectra output, and fragmentation patterns. Biomarker proxies and indices were calculated to identify biomarker sources and study environmental changes. Biomarker concentrations were quantified using known concentrations of internal standard and were normalised to the TOC content of the sediment. The carbon preference index for fatty acids (CPI), which indicates the amount of microbial activity or amount of modification (Kalpana et al., 2021), was calculated for each sample using Eq. (1).



$$CPI = \frac{\sum C_{12-28(\text{even})}}{\sum C_{13-29(\text{odd})}}, \quad (1)$$

165 Average chain length (ACL), which indicates the dominant plant source, e.g. terrestrial plant material/ocean algae, was calculated using the concentrations of saturated fatty acids following Eq. (2):

$$ACL_{14-32} = \frac{\sum (C_n \times n)}{\sum C_n}, \quad (2)$$

The $C_{16:1\omega7}/C_{16:0}$ ratio was calculated to identify diatom sources (Nichols et al., 1993; Nichols et al., 1986; Skerratt et al., 1995; Skerratt et al., 1998; Smik, Belt, et al., 2016; Smith et al., 1986). The C_{15} fatty acid index indicates levels of microbial activity
 170 and was calculated following Eq. (3):

$$C_{15} \text{ fatty acid index} = \frac{(iC_{15} + aC_{15})}{C_{15}}, \quad (3)$$

IPSO₂₅ was quantified using an internal standard and normalised to TOC. The phytoplankton IPSO₂₅ index (PIPSO₂₅) was calculated using brassicasterol (P_BIPSO₂₅) and dinosterol (P_DIPSO₂₅) following nomenclature and Eq. (4) by Vorrath et al. (2019):

$$175 \text{ PIPSO}_{25} = \frac{\text{IPSO}_{25}}{\text{IPSO}_{25} + (c \times \text{phytoplankton marker})}, \quad (4)$$

The balance factor is applied to account for concentration differences between IPSO₂₅ and the phytoplankton biomarker ($c = \text{mean IPSO}_{25}/\text{mean phytoplankton biomarker}$) (Belt & Müller, 2013; Smik, Cabedo-Sanz, et al., 2016; Vorrath et al., 2019). C factors were calculated individually for each core site.

2.6 Diatom assemblages

180 Quantitative diatom slides were prepared following Crosta et al. (2020) at Environnements et Paléoenvironnements Océaniques et Continentaux (EPOC), University of Bordeaux, to investigate diatom composition and abundances. Briefly, a subsample of dried sediment was immersed in a hydrogen peroxide and anhydrous tetra sodium pyrophosphate solution on a hotplate until reaction with organic matter was complete. The samples were centrifuged, diluted, and one drop was transferred onto a coverslip immersed in a petri dish. The water was decanted, and the dry coverslip was then glued on a slide using
 185 NOA61. Diatom analysis was performed on an Olympus BH2 phase contrast photomicroscope at a magnification of x1000. Two slides were made per sample, and at least 300 diatom valves were counted per sample across the two slides following the method outlined by Crosta and Koç (2007). Diatoms were identified to species level where possible, or species group level, following the taxonomic criteria detailed in (e.g. Al-Handal & Wulff, 2008; Almandoz et al., 2008; Andreoli et al., 1995; Baldauf & Barron, 1991; Saggiomo et al., 2021; Warnock & Scherer, 2015). The relative abundance of each species/group
 190 was determined as the proportion of the species/group to the whole diatom assemblage in each sample.

2.6 Proxy rationale

To differentiate between phytoplankton and microbial sources in the southwestern Ross Sea, we applied a multi-proxy biomarker approach incorporating fatty acid profiles, highly branched isoprenoids (HBIs), sterols, and diatom assemblages. This framework enables us to distinguish between pelagic and sympagic diatom communities, sea ice-associated taxa, *P. antarctica*, and bacterial inputs. While saturated fatty acids are produced by most organisms, variations in chain length and relative dominance can indicate source differences. A predominance of C_{16:0} is commonly associated with diatoms (Nichols et al., 1986; Skerratt et al., 1995; Smik, Belt, et al., 2016), while C_{18:0} and unsaturated C₁₈ fatty acids such as C_{18:1ω9} are more characteristic of *P. antarctica* as shown by natural blooms and pure culture studies (Hamm et al., 2001; Nichols et al., 1986; Skerratt et al., 1995; Skerratt et al., 1998). However saturated fatty acids are less diagnostic as they have multiple sources and can be derived from the degradation of unsaturated compounds. Diatom dominated assemblages also exhibit elevated concentrations of C_{16:1ω7} and polyunsaturated fatty acids (PUFAs) such as C_{20:5ω3} and C_{20:4ω15}, as well as high C_{16:1ω7}/C_{16:0} ratios, as shown by natural diatom blooms across Antarctica (Nichols et al., 1986; Skerratt et al., 1995; Smik, Belt, et al., 2016). Sea ice dwelling diatom communities from cultures and Ross Sea samples are further distinguished by long-chain monounsaturated fatty acids, including C_{24:1ω11}, C_{24:1ω9}, C_{26:1ω11}, and C_{26:1ω9} (Nichols et al., 1993; Nichols et al., 1986). Although diatom cultures contain C_{20:1ω9} (Skerratt et al., 1998), this compound is also associated with zooplankton (copepod) (Yang et al., 2016) (Zhang et al., in review). Bacterial contributions are inferred from branched-chain fatty acids, particularly iso- and anteiso- C_{15:0} and C_{17:0}, which occur in pairs (Kaneda, 1991; Skerratt et al., 1995). In additions, C_{18:1ω7} is produced by several bacterial taxa (Wilson et al., 2010). These patterns, summarised in Table 2, provide a basis for interpreting fatty acid distributions in terms of source inputs.

The HBI biomarker IPSO₂₅ diene is used across the Southern Ocean to reconstruct paleo Antarctic sea ice (Belt, 2018; Etourneau et al., 2013; Johnson et al., 2021; Lamping et al., 2020; Lamping et al., 2021; Sadatzki et al., 2023; Schmidt et al., 2018; Tesi et al., 2020; Vorrath et al., 2023; Vorrath et al., 2020), and has also been used in conjunction with two open-water biomarkers, two sterols, brassicasterol (24-methylcholesta-5,22E-dien-3β-ol) and dinosterol (4α,23,24trimethyl-5α-cholest-22E-en-3β-ol) (Smik, Cabedo-Sanz, et al., 2016). In the Southern Ocean, the index has been identified as PIPSO₂₅ by Vorrath et al. (2019) and has been used around the Bransfield Strait (Lamping et al., 2021; Vorrath et al., 2023; Vorrath et al., 2020), the Amundsen Sea (Lamping et al., 2020), and near Wilkes Land (Sadatzki et al., 2023). In Antarctic seawater and sediment, high concentrations of brassicasterol were associated with *P. antarctica* blooms (Skerratt et al., 1995; Villinski et al., 2008), consistent with the high concentrations of brassicasterol found in *Phaeocystis* cultures (Nichols et al., 1991). However, brassicasterol is also produced by certain pennate diatoms (Rampen et al., 2010) and has been found to correlate with sea ice diatom abundance and spring sea ice extent (Guo et al., 2024). Dinosterol, although occasionally detected in diatom blooms (Skerratt et al., 1995), is primarily produced by dinoflagellates and is considered a source-specific indicator of this group (Skerratt et al., 1995; Thomson et al., 2004; Villinski et al., 2008; Volkman, 2006; Wisnieski et al., 2014). However, the southwestern Ross Sea is dominated by diatoms rather than (Arrigo et al., 2000; Arrigo et al., 2015; McMinn et al., 2010;



225 Noble et al., 2013) which may lead to a larger diatom source of dinosterol. We use these biomarkers to investigate the sources and environmental drivers of phytoplankton-derived compounds in our surface samples, as well as to interpret downcore changes in sea ice extent using HBI concentrations and sterol-based ratios.

To complement biomarker analysis, as assessed diatom assemblages grouped by ecological preference following Crosta et al. (2004). *Fragilariopsis curta*, *Fragilariopsis cylindrus*, and *Fragilariopsis vanheurckii* were grouped into the *F. curta* group. High abundances of this group tracks the presence of heavy fast or pack ice, with melting late in the year (Armand et al., 2005).
 230 *Fragilariopsis obliquastata*, *Fragilariopsis sublinearis*, and *Fragilariopsis ritscherii* were grouped into the *F. cryophilic* group, which indicates the presence of sea ice in spring (Gersonde & Zielinski, 2000). The Sea Ice diatom group contained five species found within sea ice: *Entomoneis* spp., *Nitzschia stellata*, *Synedropsis fragilis*, *Synedropsis recta*, and *Synedropsis hyperboreoides* showing seeding from the melting sea ice (Leventer & Dunbar, 1988). Terminal and intercalary valves of *Eucampia antarctica* var *antarctica* were grouped together into the *E. antarctica* group. *Eucampia antarctica* is generally
 235 associated with meltwater from melting ice (Barbara et al., 2016; Burckle, 1984; Peck et al., 2015). The Centric Cold Water group contained the species *Actinocyclus actinochilus*, *Shionodiscus ritscheri*, *Stellarima microtrias*, and *Thalassiosira tumida* that develop in turbulent cold waters during the summer ice-free season (Cunningham & Leventer, 1998). The Open Ocean group contained several species that were in low abundance: *Actinocyclus curvatulus*, *Asteromphalus hookeri*, *Asteromphalus hyalinus*, *Asteromphalus parvulus*, *Corethron cryophilum*, *Coscinodiscus oculus-iridis*, *Shionodiscus gracilis*, *Shionodiscus trifulta*,
 240 *Thalassiosira lentiginosa*, *Thalassiosira maculata*, *Thalassiosira oliverana*, *Thalassiothrix* spp., and *Trichotoxon reinboldii*. This group depicts warmer conditions and a longer ice-free season (Crosta et al., 2005). Together, these assemblages were used alongside biomarker evidence to reconstruct spatial patterns in phytoplankton community structure and infer recent environmental changes in the southwestern Ross Sea.



245 **Table 2: Diagnostic lipid biomarkers reported for diatoms, *Phaeocystis antarctica*, and bacteria in Antarctic studies. Some compounds are included more than once as they represent several types of phytoplankton. MUFA = Monounsaturated fatty acids. PUFA = Polyunsaturated fatty acids.**

Potential sources	Type evidence	of	Compound type	Specific compound or ratio	Reference
Pelagic diatoms	Surface sediments		Saturated fatty acids	C _{14:0} , C _{16:0}	(Smith et al., 1986)
	Surface sediments		MUFAs	C _{16:1ω7}	(Smith et al., 1986)
	Surface sediments		PUFAs	C _{16:3ω4} , C _{20:5ω3} , C _{20:4ω6} , C _{22:4ω6} , C _{22:5ω3} , C _{22:6ω3}	(Smith et al., 1986)
	Surface sediments		High ratio	C _{16:1ω7} /C _{16:0}	(Smith et al., 1986)
	Seawater particulates		Saturated fatty acids	C _{14:0} , C _{16:0}	(Nichols et al., 1993; Nichols et al., 1986; Skerratt et al., 1995; Wing et al., 2012)
	Seawater particles		MUFAs	C _{16:1ω7} , C _{24:1ω9} , C _{24:1ω11}	(Nichols et al., 1993; Nichols et al., 1986; Skerratt et al., 1995; Wing et al., 2012)
	Seawater particles		PUFAs	C _{16:4ω1} , C _{20:5ω3} , C _{20:4ω6}	(Nichols et al., 1993; Nichols et al., 1986; Skerratt et al., 1995; Wing et al., 2012)
	Seawater particulates		High ratio	C _{16:1ω7} /C _{16:0}	(Nichols et al., 1993; Nichols et al., 1986; Skerratt et al., 1995; Wing et al., 2012)
	Phytoplankton cultures		Sterols	Brassicasterol, dinosterol	(Rampen et al., 2010)
Sea ice dwelling diatoms	Seawater/ice particulates		MUFAs	C _{24:1ω9} , C _{24:1ω11} , C _{20:1}	(Fahl & Kattner, 1993; Nichols et al., 1986)
	Seawater/ice particulates		Highly branched isoprenoids (HBI)	Di-unsaturated C ₂₅ HBI alkene (IPSO ₂₅ diene; Ice Proxy Southern Ocean)	(Smik, Belt, et al., 2016)
	Sediments		Highly branched isoprenoids	IPSO ₂₅ diene	(Belt, 2018)
	Sea ice		Highly branched isoprenoids	IPSO ₂₅ diene	(Belt et al., 2016)
<i>Phaeocystis antarctica</i>	Seawater particulates		Saturated compounds	C _{14:0}	(Skerratt et al., 1995)
	Seawater particulates		PUFAs	Low levels	(Skerratt et al., 1995)
	Seawater particulates		Low ratio	C _{16:1ω7} /C _{16:0}	(Skerratt et al., 1995)



	Seawater particulates	Sterols		Brassicasterol	(Skerratt et al., 1995)
	Sediments	Saturated acids	fatty	C _{18:0}	(Ashley et al., 2021)
	Sediments	Sterols		Brassicasterol	(Villinski et al., 2008)
	Phytoplankton cultures	Sterols		Brassicasterol	(Nichols et al., 1991)
	Phytoplankton cultures	Saturated compounds		C _{14:0} , C _{16:0} , C _{18:0}	(Nichols et al., 1991; Skerratt et al., 1998)
	Phytoplankton cultures	MUFAs		C _{18:1ω9}	(Nichols et al., 1991; Skerratt et al., 1998)
Bacteria	Surface sediments	MUFAs		C _{18:1ω7}	(Smith et al., 1986)
	Surface sediments	Branched acids	fatty	iC _{14:0} , iC _{15:0} , αC _{15:0} , iC _{17:0} , αC _{17:0}	(Skerratt et al., 1995; Smith et al., 1986)

3 Results

3.1 Biomarkers

250 Fatty acids were the most abundant biomarkers in the studied sediments, and the results reported here focus on fatty acids diagnostic of different phytoplankton groups (see section 2.6). Analysis of the fatty fraction identified 44 saturated and unsaturated compounds with carbon chain lengths between C₁₂-C₃₀, exhibiting a pronounced even-over-odd carbon number predominance (Figure 2). Saturated fatty acids dominated the samples, with C_{14:0} and C_{16:0} showing the highest concentrations compared to longer-chain fatty acids. Monounsaturated fatty acids were also abundant within the C₁₄-C₁₈ range, with C_{16:1} and

255 C_{18:1ω7} showing the highest concentrations. Branched fatty acids comprise between 8 % and 20 % of total fatty acids. Average chain length (ACL) of C₁₂-C₃₀ fatty acids ranged between 16.1 and 19.2 (mean = 17.8; Table 3). The C₁₅ fatty acid index ranged from 3 to 8.7 across cores. Spatially, ACL increased from south to north along the transect, with BC02 displaying the lowest and BC04 the highest values, whereas ratios of C_{16:1ω7}/C_{16:0} were consistent across cores. The proportion of branched saturated fatty acids increases from north (BC04; 11.5%) to south (GC72; 19%), with the central core tops containing similar proportions

260 of ~15% (Table 3). However, the C₁₅ index was similar across cores. Relative abundances of fatty acid compounds were broadly consistent across surface sediment samples, with small variations in C_{14:0}, C_{18:0} and C₁₆ compounds which vary across core tops, without any distinct spatial pattern. C_{24:0} increased on a south-to-north gradient, and C_{18:1ω9} was least concentrated towards the southern end of the transect (Figure 4). Downcore, total fatty acid concentrations decreased exponentially, declining by ~50 % between 1-30 cm depth before stabilising toward the base of the cores (Figure 3). The C₁₅ index also

265 decreased with depth. Decay rates for target compounds, calculated from TOC-normalised fatty acid concentrations, ranged



from ~ 22 to 93 ng cm^{-1} for the first 20 cm, after which compounds have reached the asymptote. The lowest decay rates are observed in higher chain length saturated fatty acids $\text{C}_{18:0}$ and $\text{C}_{24:0}$ ($22\text{--}36 \text{ ng cm}^{-1}$). Decay rates for saturated, unsaturated, and branched fatty acids with chain lengths lower than C_{18} are between 46 and 93 ng cm^{-1} . All three sediment cores demonstrate similar decay rates over similar depths (Figure 3).

270

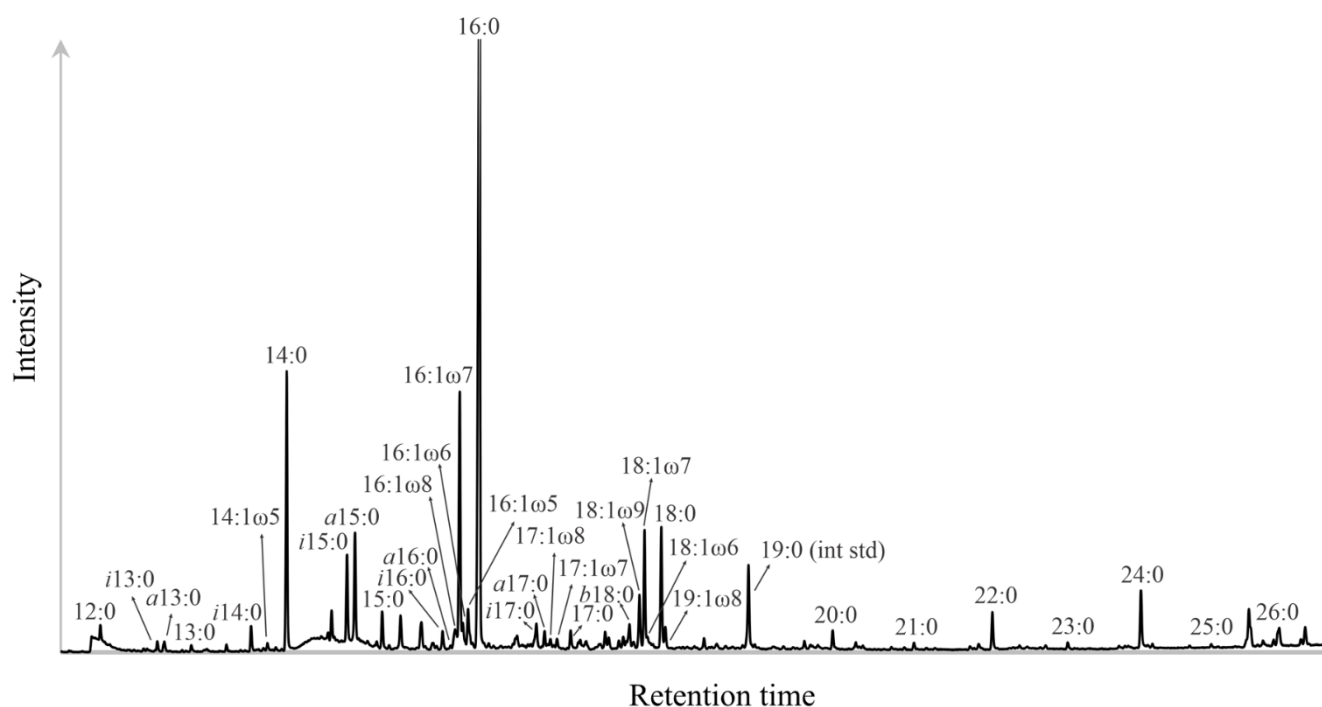


Figure 2: Representative chromatogram of the fatty acid fraction of a typical southwestern Ross Sea sediment sample (BC02; 11-12cm). Identified compounds are annotated by carbon number, number of double bonds, and ω -position of double bonds. Abbreviations: i = iso, a = anteiso, b = branched.



275

Table 3: Chemical composition of southwestern Ross Sea sediment cores including bulk sediment characteristics (TOC and C/N), HBIs (IPSO25), absolute diatom abundance expressed as valves per gram dry weight (v gdw⁻¹) and relative species abundance (Chaetoceros resting spores (CRS), Fragilariopsis curta (F. curta), Fragilariopsis cylindrus (F. cylindrus), Thalassiosira antarctica cold (T. antarctica)), fatty acids (average chain length (ACL12-30), total fatty acids (Total FA), C15 fatty acid index, ratio of C16:1ω7/C16:0, and percent of branched fatty acids).

Core	Depth (cm)	TOC (wt %)	C/N	IPSO ₂₅ (μg g ⁻¹ TOC)	Diatom abundance (v gdw ⁻¹)	Chaetoceros RS (%)	F. curta (%)	F. cylindrus (%)	T. antarctica (%)	ACL ₁₂₋₃₀	Total FA (μg g ⁻¹ TOC)	iC ₁₅ /aC ₁₅	C _{16:1ω7} /C _{16:0}	Branched fatty acids (%)
BC02	1-2	1.7	7.0	57.3	285×10 ⁶	21.2	49.3	0.9	9.3	16.8	1737.2	7.2	0.33	15.5
	5-6	1.7	7.0	35.6	282×10 ⁶	21.3	46.1	1.1	12.2	16.2	1447.8	6.8	0.36	16.9
	11-12	1.6	7.0	31.1	251×10 ⁶	21.1	50.6	0.0	10.2	16.5	1233.6	4.9	0.25	15.5
	15-16	1.8	7.3	41.3	323×10 ⁶	17.3	46.2	0.2	10.8	16.7	1358.3	6.1	0.22	17.5
	21-22	2.1	8.4	7.3	276×10 ⁶	19.6	47.6	0.7	9.7	17.3	751.4	4.2	0.19	12.0
	25-26	2.2	8.4	20.0	302×10 ⁶	23.2	48.7	2.4	9.0	18.1	788.7	4.7	0.20	13.7
	31-32	1.7	8.2	9.0	218×10 ⁶	29.8	41.3	1.4	8.5	17.5	537.4	3.2	0.13	8.9
	35-36	1.6	7.8	14.2	488×10 ⁶	22.6	46.5	2.4	11.1	17.5	790.1	3.6	0.16	10.5
BC03	1-2	1.8	7.1	18.3	234×10 ⁶	14.3	52.8	3.9	9.0	17.3	1735.1	6.8	0.48	15.3
	7-8	1.9	7.3	29.8	236×10 ⁶	13.3	57.4	0.6	11.0	17.6	1108.1	7.5	0.37	14.3
	13-14	1.8	7.2	46.1	310×10 ⁶	11.9	64.6	4.0	5.3	18.5	1236.9	6.9	0.32	15.9
	19-20	1.8	7.4	12.8	296×10 ⁶	13.5	63.2	1.5	6.2	17.1	1013.2	6.4	0.19	19.4
	25-26	1.7	7.8	12.1	282×10 ⁶	18.2	58.6	1.5	6.8	17.7	900.6	6.4	0.25	18.0
	31-32	1.7	7.7	4.4	223×10 ⁶	12.4	57.1	4.8	9.3	17.6	946.9	6.2	0.25	18.5
	37-38	1.7	7.1	6.1	241×10 ⁶	15.3	57.1	4.6	5.5	17.7	1036.1	5.8	0.28	19.5
	43-44	1.5	7.2	4.8	273×10 ⁶	11.7	58.4	2.1	7.5	18.7	982.7	3.0	0.11	9.1
BC04	1-2	2.1	6.8	53.0	421×10 ⁶	12.9	64.5	5.4	4.3	18.4	1632.4	8.6	0.29	11.5
	7-8	1.8	6.8	29.8	224×10 ⁶	10.0	58.9	2.6	8.0	18.1	1269.6	5.7	0.40	14.2
	15-16	1.8	7.0	18.0	156×10 ⁶	11.9	65.3	4.0	4.9	18.9	1029.6	5.9	0.30	12.2
	21-22	2.0	6.8		192×10 ⁶	14.4	60.8	3.8	5.3	19.2	803.0	5.8	0.27	13.8
	29-30	2.0	6.9	8.6	97×10 ⁶	14.8	56.8	1.0	10.0	18.4	575.7	4.2	0.19	11.3
	35-36	1.8	6.8	10.7	194×10 ⁶	16.6	45.1	12.1	6.3	17.9	715.7	4.6	0.16	13.9
	43-44	2.1	6.6	5.1	143×10 ⁶	21.6	52.0	1.5	8.2	18.2	529.4	3.5	0.15	7.9
	49-50	1.9	6.9	4.7	167×10 ⁶	26.9	43.9	3.2	6.6	18.4	767.0	3.9	0.23	13.2
GC72	0-1	1.8	7.0	32.6	150×10 ⁶	21.1	48.0	2.5	4.3	16.7	1273.6	8.7	0.68	19.0
GC78	0-1	1.9	6.7	27.9	202×10 ⁶	21.8	50.6	2.6	10.6	16.7	2239.9	6.1	0.81	14.8
GC80	0-1	1.8	7.0	17.8	206×10 ⁶	25.5	46.0	2.6	10.3	17.1	1665.1	5.8	0.47	14.0

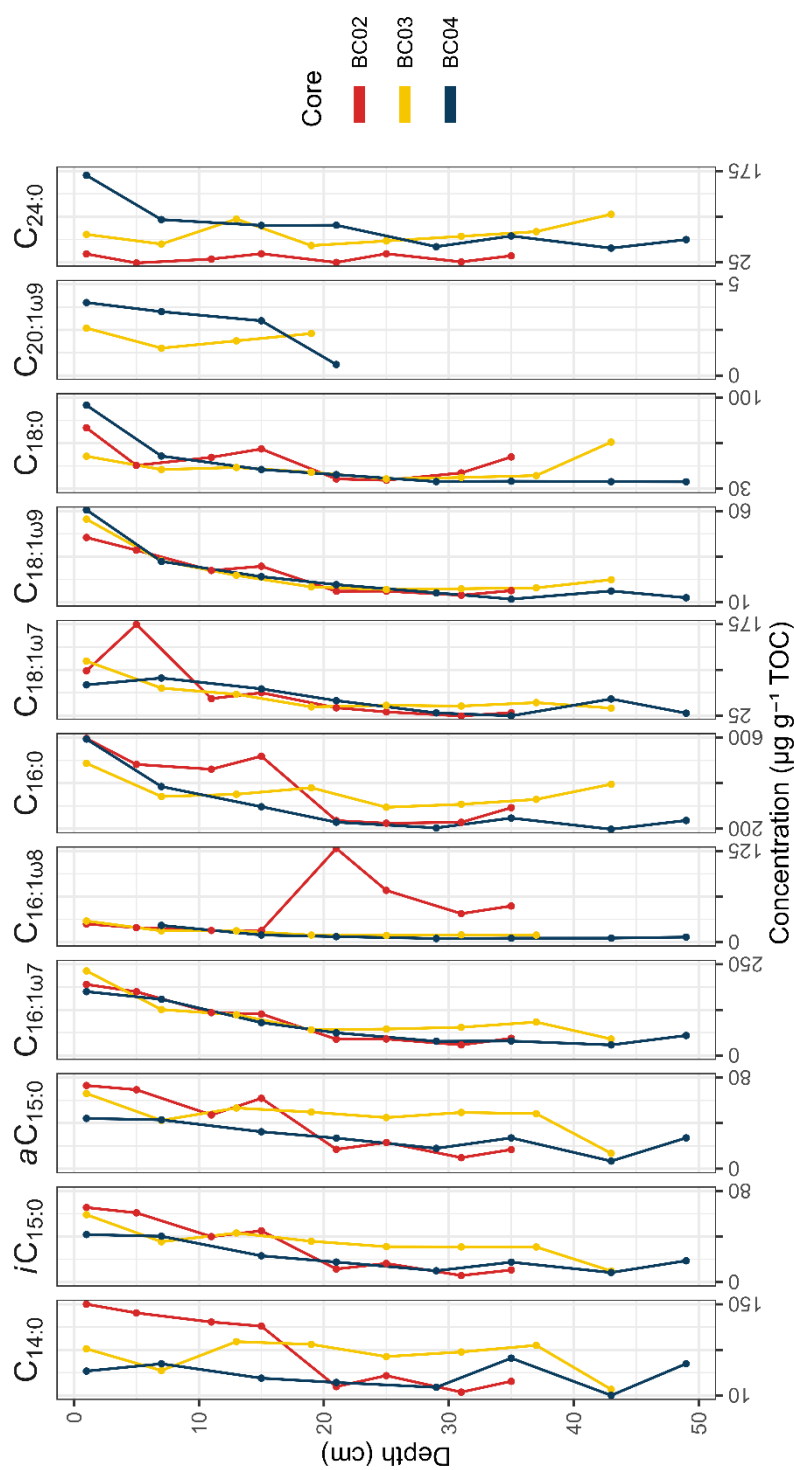


Figure 3: Fatty acid concentrations of saturated and unsaturated fatty acids (C_{14} – C_{24}) in the sediment cores vs depth.

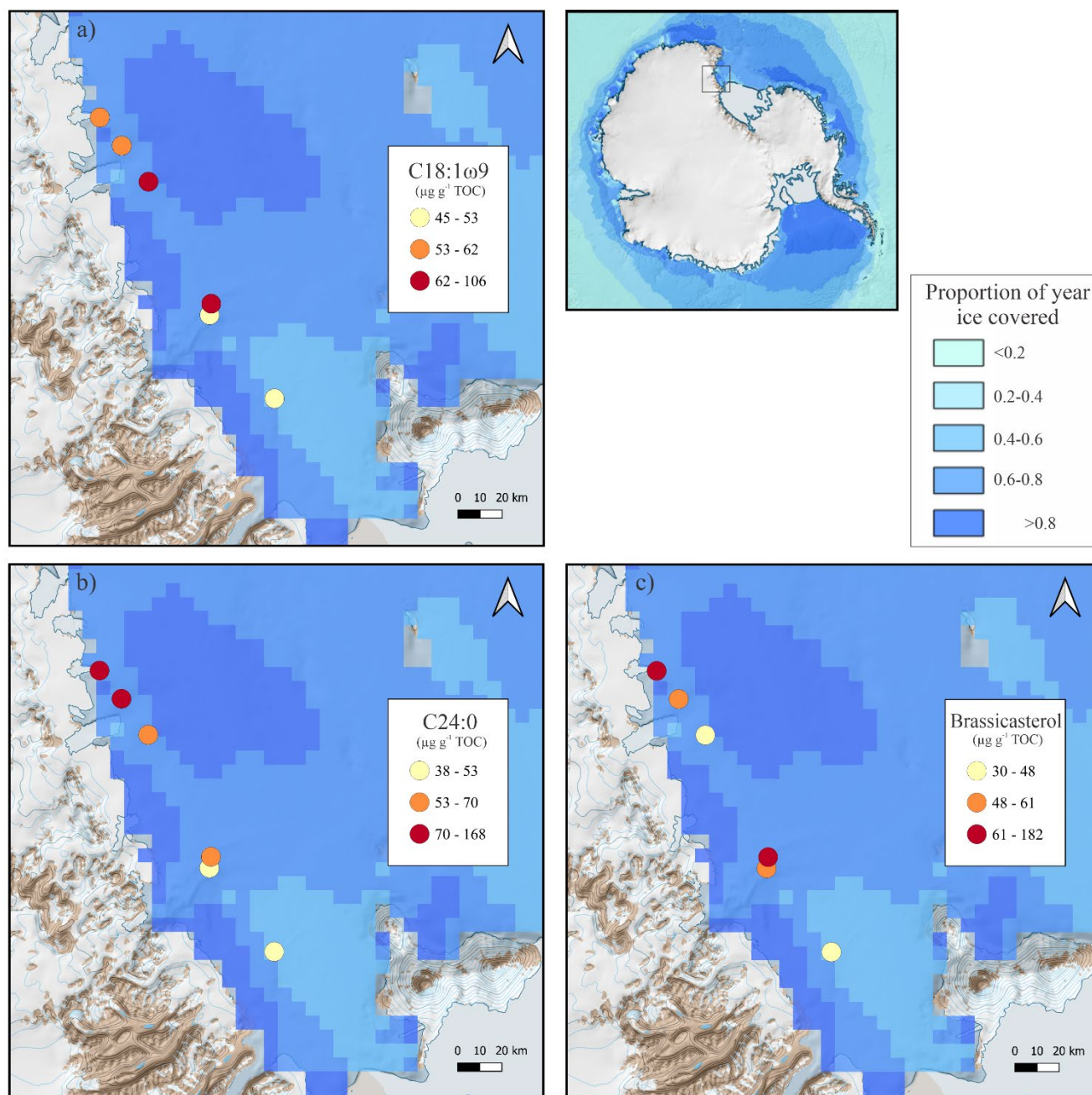


Figure 4: Spatial distribution of select phytoplankton derived biomarkers in core top sediments (0-2 cm depth). (a) C18:1ω9, (b) C24:0, and, (c) brassicasterol. Areas with lighter blue colours have open water more often throughout the year, whereas dark blues are covered with sea ice for most of the year based on sea ice concentration data between 2002 and 2011 at 6.25 km resolution. Base map sourced from Quantarctica (Matsuoka et al., 2021). Sea ice data source: Spreen et al. (2008).



Sterols, namely brassicasterol and dinosterol, were present in all sediment samples. Brassicasterol concentrations ranged
 280 between 19 and 182 $\mu\text{g g}^{-1}$ TOC, while dinosterol ranged between 8 and 50 $\mu\text{g g}^{-1}$ TOC. Although core tops show substantial
 differences in absolute concentrations, no clear spatial pattern is evident (Figure 4). BC04 contained the highest core-top
 concentrations of both brassicasterol (182 $\mu\text{g g}^{-1}$ TOC) and dinosterol (50 $\mu\text{g g}^{-1}$ TOC), whereas the other sites ranged between
 30–77 $\mu\text{g g}^{-1}$ TOC for brassicasterol and 9–36 $\mu\text{g g}^{-1}$ TOC for dinosterol. Downcore trends differ from those of fatty acids
 (Figure 7): brassicasterol decreases with depth before increasing again, whereas dinosterol increases within the upper 15–20
 285 cm and then declines.

Highly branched isoprenoids (HBIs) in the southwestern Ross Sea display both spatial and downcore variability. IPSO₂₅ diene
 was present in all sediment samples except one (BC04 21–22 cm), and concentrations vary across core tops between 17.8 and
 57.3 $\mu\text{g g}^{-1}$ TOC. BC04, despite its proximity (<25 km) to BC03, has 52.9 $\mu\text{g g}^{-1}$ TOC of IPSO₂₅ diene in the core top, compared
 to BC03 with 18.3 $\mu\text{g g}^{-1}$ TOC. BC02, which is 100 km away from BC04, has similar concentrations of IPSO₂₅ diene, 57.3 $\mu\text{g g}^{-1}$
 290 $\mu\text{g g}^{-1}$ TOC. The two northern cores (BC04 and BC03) located near each other demonstrate similar P_BIPSO₂₅ and P_DIPSO₂₅ values.
 Like fatty acid concentrations, IPSO₂₅, P_BIPSO₂₅ and P_DIPSO₂₅ decrease with increasing sediment depth (Figure 5). IPSO₂₅
 diene decreases by ~70 % between the sediment surface and 30 cm depth, below which it remains constant. The asymptote of
 IPSO₂₅ diene is ~20–30 cm in all three sediment cores (Figure 5). The decay rate of IPSO₂₅ calculated from TOC-normalised
 concentrations ranges from ~30–60 ng cm⁻¹ in BC02, BC03, and BC04 over the first 20–30 cm, below which concentrations
 295 remain relatively stable. Overall, all three cores demonstrate a decreasing downcore trend except for decreased IPSO₂₅ diene
 in surface sediment from BC03 (Figure 5).

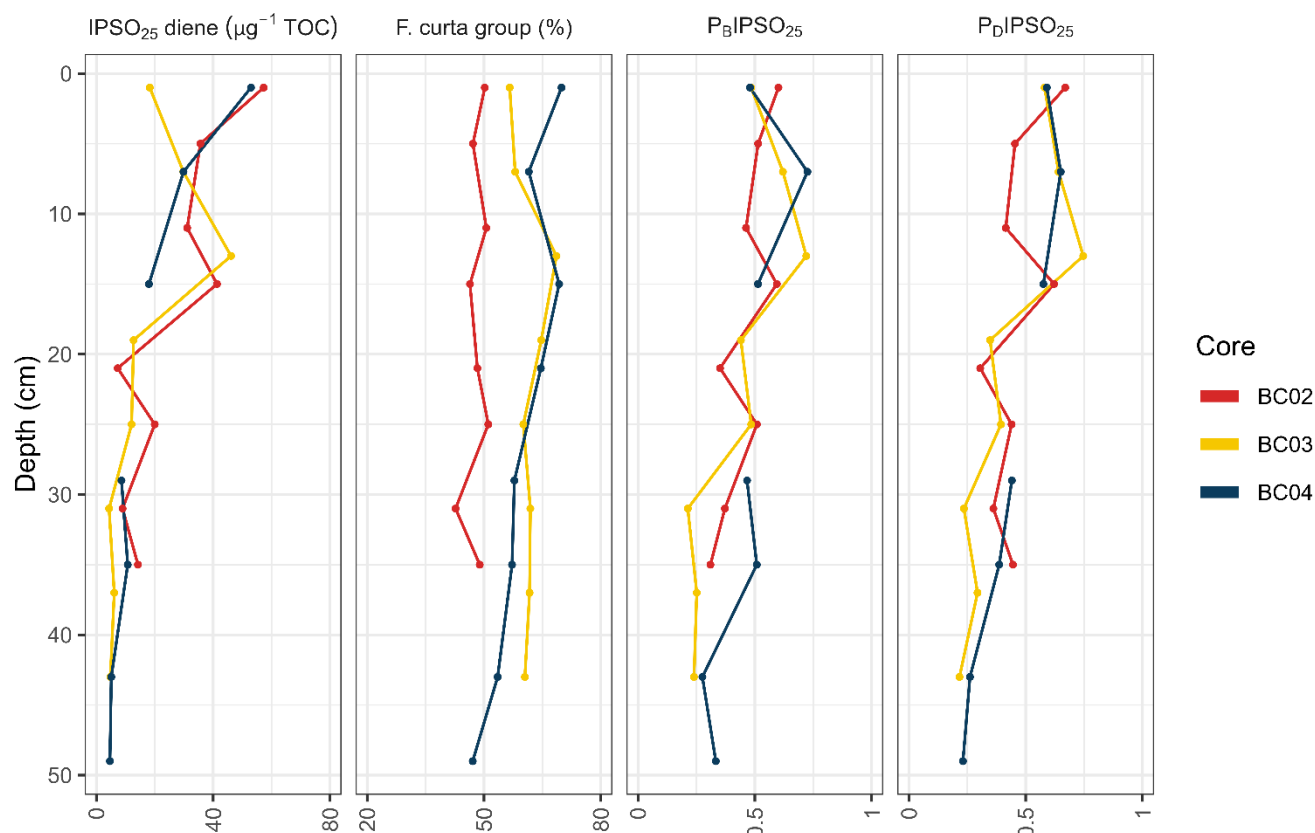


Figure 5: IPSO₂₅ diene concentrations relative to total organic carbon (TOC), per cent of *Fragilariopsis curta* (*F. curta*) group, and PIPSO ratios (P_BIPSO₂₅ and P_DIPSO₂₅) in the sediment cores vs depth.

300 3.2 Diatom composition

Fifty-eight species or groups of species were identified in the sediment samples. The diatom assemblage in all the sediment samples is characterised by high abundances of *Fragilariopsis curta*, *Chaetoceros* resting spores (CRS), *Thalassiosira antarctica* cold, and *Fragilariopsis cylindrus* (Figure 7). The diatom abundance is expressed as valves per gram dry weight (v gdw⁻¹), and ranges from 97×10⁶ v gdw⁻¹ to 488×10⁶ v gdw⁻¹ across the sediment samples. Diatom abundances and species
 305 vary spatially. Diatom abundance decreases northward, with the highest diatom abundance observed in the core top of BC02 (303 ± 76 × 10⁶ v gdw⁻¹), followed by BC03 (262 ± 30 × 10⁶ v gdw⁻¹), and the lowest abundance seen in BC04 (199 ± 91 × 10⁶ v gdw⁻¹). To assess sea ice and phytoplankton variability, spatial variation in ‘centric cold-water diatoms’, CRS, and *F. curta* were compared to the average proportion of sea ice cover across the southwestern Ross Sea from 2002-2011 (Spreen et al., 2008), covering the time represented by the core tops (Figure 6). Relative proportions of ‘centric cold-water diatoms’
 310 decrease northward away from the McMurdo biological hotspot, whereas proportions of *F. curta* are highest towards the north. CRS, similar to the ‘centric cold-water diatoms’, decrease on a south-to-north gradient, away from the polynya. Diatom



concentration downcore varies between the three box cores. BC04 show decreasing abundance of diatoms downcore, while BC02 and BC03 have a relatively stable diatom abundance downcore (Figure 7). Diatom concentration downcore varies between the three box cores. BC04 show decreasing abundance of diatoms downcore, while BC02 and BC03 have a relatively stable diatom abundance downcore (Figure 7). The *F. curta* group dominates the diatom assemblage across the record and ranges from 42% to 70% of all diatoms counted but decreases downcore consistently in all three cores (Figure 7). CRS shows the opposite trend and increases downcore (Figure 7), with average proportions of 14% to 22% in the three box cores. *Thalassiosira antarctica* represent on average ~8% of all diatoms counted, and no clear downcore trend is observed. Similarly, the *F. cyrophilic* group, the open ocean group, sea-ice group, centric cold water group, and *E. antarctica* do not demonstrate a strong increasing or decreasing trend (Figure 7).

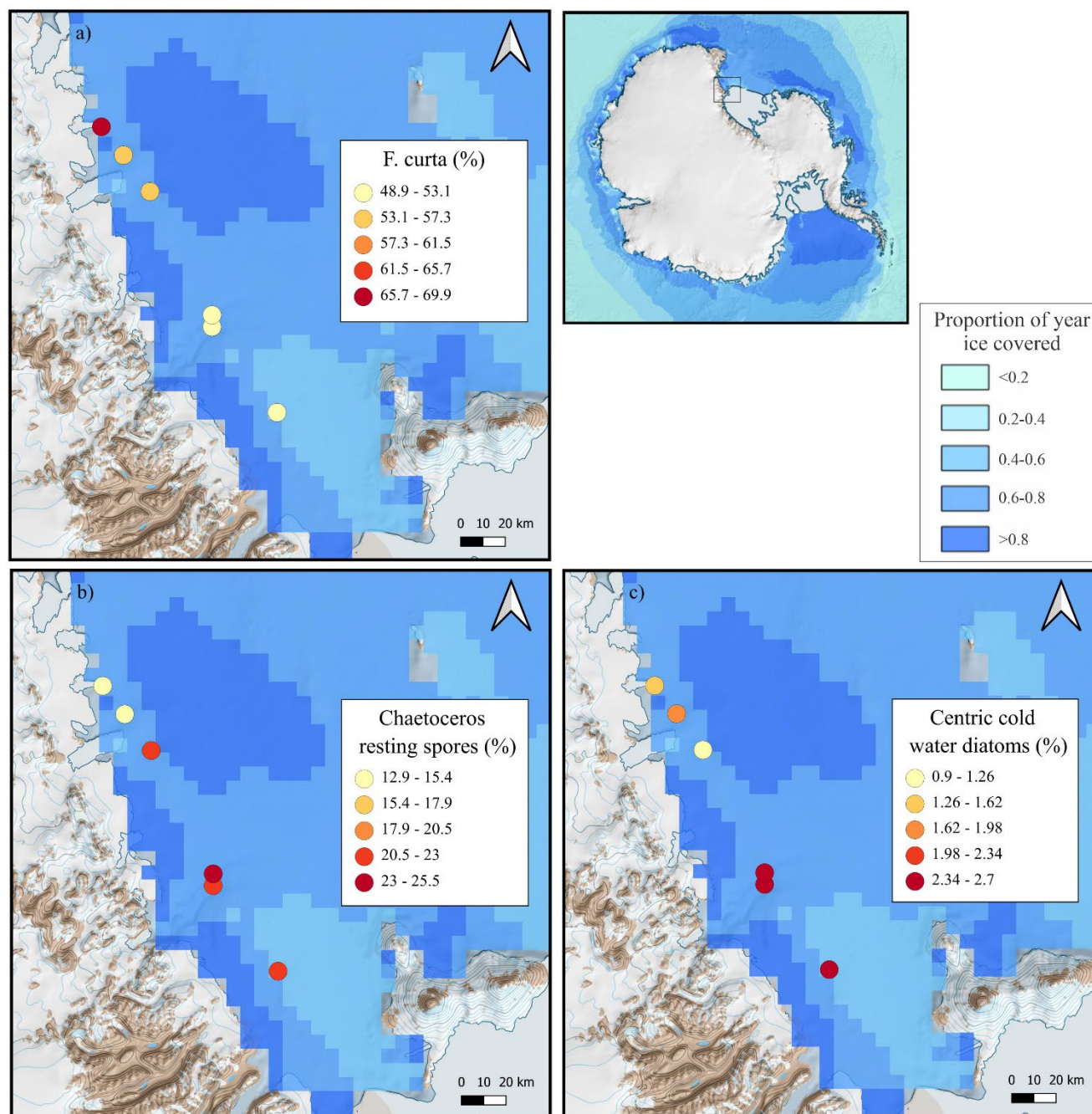


Figure 6: Relative diatom concentration of select species in core top sediments (0-2 cm depth). (a) *F. curta*, (b) *Chaetoceros* RS, and, (c) Centric cold water diatoms. Areas with lighter blue colours have open water more often throughout the year, whereas dark blues are covered with sea ice for most of the year based on sea ice concentration data between 2002 and 2011 at 6.25 km resolution. Base map sourced from Quantarctica (Matsuoka et al., 2021). Sea ice data source: Spreen et al. (2008).

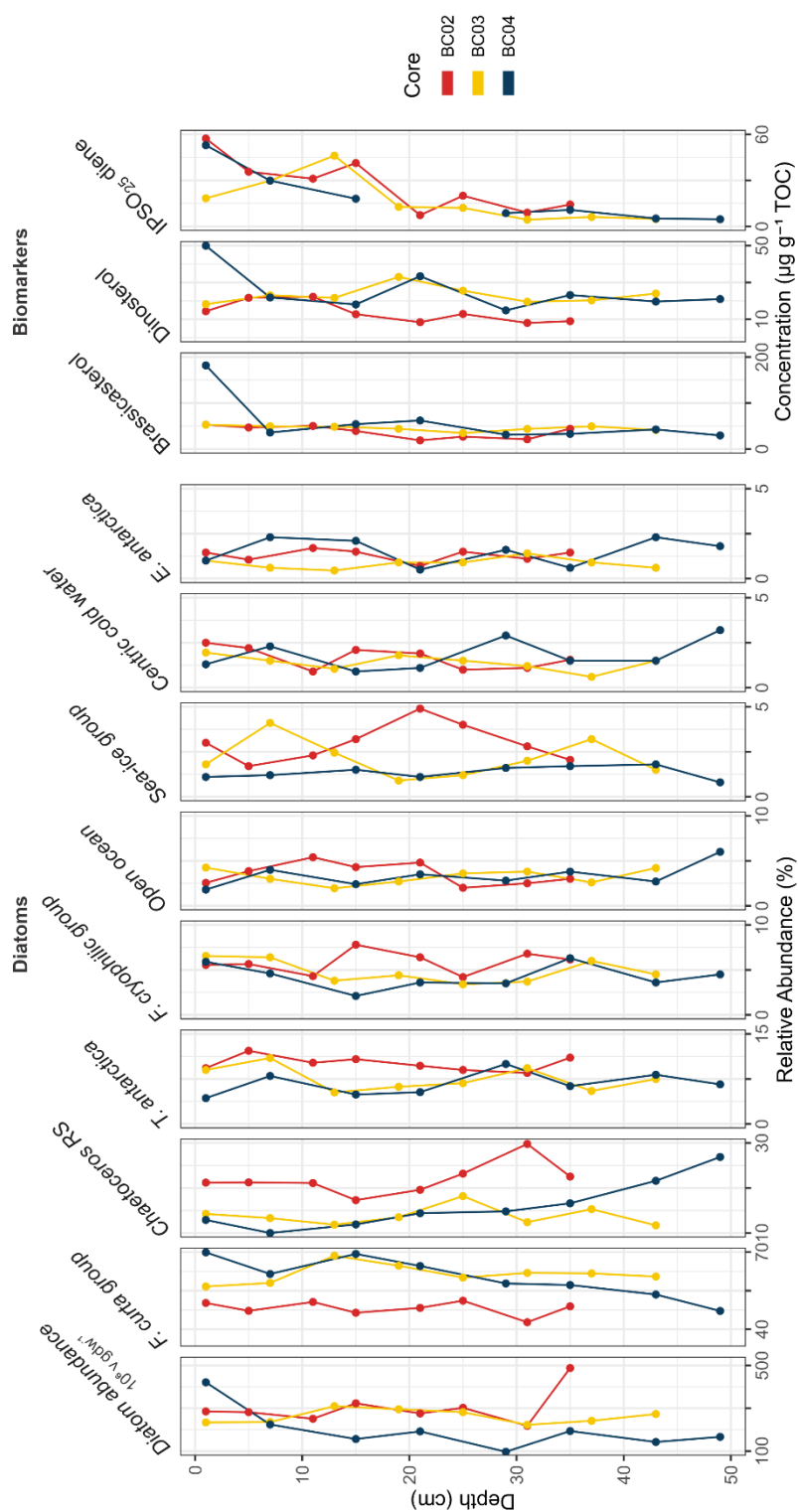


Figure 7: Discontinuous downcore relative concentrations of diatom groups (*F. curta* group, *Chaetoceros* RS, *T. antarctica*, *F. cryophilic* group, open ocean group, sea ice group, centric cold water group, *E. antarctica* group), diatom abundance, and biomarkers (Brassicasterol, Dinosterol and IPSO₂₅ diene) with depth.



330 4 Discussion

4.1 Drivers of fatty acid and highly branched isoprenoids in Ross Sea marine sediments

4.1.1 Biomarker sources

The first driver of differences in southwestern Ross Sea lipid biomarkers is the differences in sources from which they are derived. The sediment samples are dominated by marine-derived compounds. C/N ratios between 6.58-8.39 indicate a strong
 335 marine algae signal and low inputs from old terrestrial organic matter that may affect biomarker signals (Meyers, 1997). This is reinforced by low ACL of fatty acids and high concentrations of phytoplankton-sourced sterols and fatty acids (Table 3). The southwestern Ross Sea and McMurdo Sound phytoplankton communities tend to be dominated by diatoms due to the water column stratification (Arrigo et al., 2000; Arrigo et al., 2015; McMinn et al., 2010; Noble et al., 2013). However, year-to-year variability in environmental factors, such as less upper ocean water stabilisation, can result in *P. antarctica* blooms
 340 (Hayward et al., 2023; Hayward et al., 2025; Mangoni et al., 2017; Stoecker et al., 1995), as well as occasional mixed communities where diatoms bloom in the ocean's upper layer and *P. antarctica* in a deeper layer (Mangoni et al., 2017). As outlined in Section 2.6, we use a multi-parameter approach to identify the phytoplankton and sea ice algae sources of biomarkers (Table 2). We use these findings to investigate the links between biomarkers in our sediment samples and the different phytoplankton and microbial sources.

345

Pelagic diatoms:

A pelagic diatom source for biomarkers in sediment samples in this study is indicated by 1) high concentrations of C_{14:0} and C₁₆ fatty acid compounds such as C_{16:0} and C_{16:1}, and 2) relatively high concentrations of C_{16:1ω7} fatty acid. However, the ratio of C_{16:1ω7}/C_{16:0} in all 27 sediment samples was, on average, ~0.3, which is lower than other studies analysing fatty acids in
 350 Antarctic surface waters during diatom blooms from McMurdo Sound and Eastern Antarctica (Skerratt et al., 1995; Smith et al., 1986).

PUFAs (C_{16:4ω1}, C_{20:5ω3}, C_{20:4ω6}), which can also be indicative of a pelagic diatom source (Nichols et al., 1993; Nichols et al., 1986; Skerratt et al., 1995; Wing et al., 2012), were not identified in the any of the studied samples despite being detected in surface sediments from locations around Ross Island (Smith et al., 1986). While it is possible that PUFAs were not produced
 355 locally due to low abundances of pelagic diatoms, the presence of pelagic diatoms preserved in our sediment suggests an alternate explanation. PUFAs may have originally been produced in the source blooms but subsequently lost in surface waters and during sinking due to several processes. First, show a strong affinity to particles and are efficiently scavenged from surface waters (REF). Second, PUFAs are highly sensitive to microbial remineralisation in the water column and sediments (Wakeham et al., 1997). Finally, PUFAs also undergo intense photo and autooxidation in the water column before reaching the seafloor
 360 (Rontani et al., 2019). Indeed, low PUFA concentrations have been observed in surface waters of East Antarctica, despite high



diatom abundances, supporting the idea of scavenging and degradation (Rontani et al., 2019; Smik, Belt, et al., 2016). The absence of PUFAs in our samples, both in core-tops and downcore sediments, suggests an intense degradation compared to previous studies (Smith et al., 1986), as supported by the presence of more bacterial markers and higher C_{15} index values (Table 3).

365 Sea ice dwelling diatoms:

The biomarker results indicating a sea ice diatom presence in this study are 1) high concentrations of $C_{24:0}$, and 2) high concentrations of $C_{20:1\omega9}$ compounds found in sites with heavier sea ice influence. $C_{24:1\omega9}$ and $C_{24:1\omega11}$ fatty acids have been found to be diagnostic of Antarctic sea ice diatoms (Nichols et al., 1986), however, these are not found in our sediment samples. $C_{24:1\omega11}$ and $C_{24:1\omega9}$ degrade over time to $C_{24:0}$, likely inflating the concentration of $C_{24:0}$ in samples with high sources of sea ice diatoms (Rontani et al., 2019). In the six core top samples, $C_{24:0}$ increases on a south to north gradient, with inflated concentrations in areas of increased sea ice concentration (Figure 4), while downcore concentrations of $C_{24:0}$ aligns with the increased presence of sea ice-associated diatoms in the *F. curta* group, evidence for a sea ice source for these compounds (Figure 4). While acknowledging $C_{20:1}$ has multiple sources, including both sea ice diatoms and zooplankton (Fahl & Kattner, 1993; Nichols et al., 1986), $C_{20:1\omega9}$ was identified in the upper 20 cm in only BC03 and BC04 (Figure 3), reflecting again the sea ice conditions above the core site. Increased $C_{20:1\omega9}$ also aligns with increased presence of *F. curta* group downcore in BC04, but not in BC03, highlighting that $C_{20:1}$ compounds in the southwestern Ross Sea are likely sourced from both diatoms and zooplankton (Fahl & Kattner, 1993; Guo et al., 2024; Nichols et al., 1986; Yang et al., 2016).

IPSO₂₅ is dominantly sourced by the sea ice diatom *Berkeleya adeliensis* (Belt et al., 2016). *Berkeleya adeliensis* was not identified in any of the three cores studied here, despite the presence of IPSO₂₅, which is consistent with other studies around Antarctica (Tesi et al., 2020). Either IPSO₂₅ is produced by other unknown sources, not yet identified (Tesi et al., 2020), despite culture experiments (Belt et al., 2018), or *B. adeliensis* is unable to reach the sediments because of its lightly silicified valves (Moriwaki, 1990; Riaux-Gobin et al., 2011; Tesi et al., 2020).

Haptophytes:

The presence of *P. antarctica* sourced lipids in southwestern Ross Sea sediments is indicated by 1) relatively high concentrations of $C_{16:0}$ and $C_{18:0}$ and low $C_{16:1\omega7}/C_{16:0}$ ratios, 2) relatively high concentrations of $C_{18:1\omega9}$, and 3) high concentrations of brassicasterol.

In the six core top samples, $C_{18:0}$, and $C_{18:1\omega9}$ concentrations were lowest towards the southern end of the transect and higher in the middle and toward the northern end of the transect (Figure 4), suggesting a possible increase in *P. antarctica* stocks under heavier sea ice conditions. $C_{16:0}$ and $C_{18:0}$ are generic compounds synthesised by a diversity of sources. However, diatoms contain very minimal amounts of C_{18} compounds, which can be robustly attributed to *P. antarctica* sources in our study area (Nichols et al., 1993; Nichols et al., 1986; Skerratt et al., 1995; Wing et al., 2012). The southwestern Ross Sea is known to have a varied phytoplankton community spatially and temporally (Arrigo et al., 2000; Mangoni et al., 2017; McMinn et al., 2010; Noble et al., 2013; Stoecker et al., 1995). High concentrations of Brassicasterol have been found to be sourced by *P. antarctica* (Nichols et al., 1991; Rampen et al., 2010; Skerratt et al., 1995). Here, brassicasterol concentrations closely follow



395 downcore trends in the *F. curta* group, rather than open-water diatoms and CRS. This also indicates a possible increase in *P. antarctica* under heavier sea ice conditions.

Bacteria

High proportions of branched fatty acids (>9 %), the presence of branched fatty acid pairs such as iC_{15}/iC_{17} and aC_{15}/aC_{17} , as well as even-chained branched fatty acids (e.g., aC_{16}), and high C_{15} fatty acid index values indicate a significant presence of
 400 bacteria (Skerratt et al., 1995; Smith et al., 1986). $C_{18:1\omega7}$ is consistently the most abundant monounsaturated C_{18} compound, which has been attributed to a bacterial source in other Ross Sea sediment samples (Smith et al., 1986).

Branched fatty acids were present in similar proportions across core top samples (Table 3), however BC04, the southernmost site, had 65 % less branched fatty acids than BC02. This suggests elevated bacterial biomass or activity near the McMurdo biological hotspot, likely associated with higher local primary productivity.

405 4.1.2 Environmental conditions

The study sites investigated in this study are located along a north-south transect from south of the Drygalski Ice Tongue, which is covered in sea ice for ~80 % of the year, to McMurdo Sound in the south, which is covered in sea ice for around 20-40 % (Figure 1, Spreen et al. (2008)). Sea ice in the southwestern Ross Sea undergoes a dramatic change every year when the spring/summer sea ice breakup forms ice-free biological hotspots in McMurdo and Terra Nova Bay (Brett et al., 2020). Site
 410 BC02 at the southern end of the transect is closest to the McMurdo polynya, where the proportion of ice-free days is the highest. The lower sea ice duration at the BC02 site is reflected by the lowest relative abundances of the *F. curta* group, increased proportions of open ocean and centric cold water diatoms, decreased $C_{24:0}$ fatty acids sourced from sea ice diatoms (Nichols et al., 1986), and the absence of sea ice diatom-sourced $C_{20:1}$ compounds (Fahl & Kattner, 1993). Biomarker and diatom distributions in BC02 also reflect enhanced phytoplankton productivity, as fatty acid ACL is lower, the CRS
 415 concentration is increased, and the diatom absolute abundance is more than 15.8% higher relative to BC03 and BC04. The northern end of the transect (BC03 and BC04) has higher sea ice duration with a break-up later in the summer than at McMurdo Sound (Spreen et al., 2008). Increased sea ice cover is seen in our core sediments, with *F. curta* abundances being 7% and 30% higher in BC03 and BC04, respectively, than in BC02. The same trend is observable in fatty acid concentrations of $C_{24:0}$, which is likely a reflection of degraded sea ice diatom-produced $C_{24:1\omega11}$ and $C_{24:1\omega9}$ (Nichols et al., 1993; Nichols et al., 1986).
 420 BC03 and BC04 also have higher ACL, lower proportions of CRS, and lower diatom abundances, which all reflect the lower productivity in this region. Smaller proportions of open-ocean diatoms are likely the result of delayed sea ice opening above the two core locations, which influences the release of nutrients and the stratification of the water column. Overall, sea ice diatom-derived lipids, $C_{20:1}$ and $C_{24:0}$ fatty acids, IPSO₂₅ diene HBI, and brassicasterol were observed in areas with more sea ice cover (Spreen et al., 2008). Dinosterol does not follow sea ice trends and may thus be a more appropriate ‘phytoplankton’
 425 biomarker in the PIPSO₂₅ equation as already evidenced by a recent study in the Amundsen Sea (Lamping et al., 2020).



4.1.3 Degradation of biomarkers

Fatty acids in the southwestern Ross Sea decrease with sediment depth in all three box cores, indicating downcore degradation consistent with patterns commonly observed in marine sediments due to various forms of degradation such as remineralisation, biogenesis, and diagenesis (Haddad et al., 1992; Wakeham et al., 1984). The significant presence of iso and anteiso branched compounds, typical bacterial markers, suggests that bacterial degradation plays an important role in these downcore changes (Skerratt et al., 1995). This is further supported by the high C₁₅ fatty acid index values (Table 3). Understanding these degradation processes is crucial for interpreting depth profiles and temporal patterns within each core. In our sediment cores, the decline of fatty acids is most notable in the top 10 cm of the sediment cores, with asymptote occurring ~20 cm (or 76-95 years). Sediment cores from Adélie Land, the only other Antarctic study analysing high-resolution temporal trends in Antarctic fatty acids over the last 2000 years, observe the same degradation patterns, with fatty acid concentrations asymptote occurring at a depth of >30-40 cm and the highest concentrations occurring in the top 80 cm (or 70 years) (Ashley et al., 2021). However, Ashley et al. (2021) did not report any unsaturated or branched fatty acids. This suggests that degradation occurred in the surface waters and/or throughout the 1000 m water column before deposition (Ashley et al., 2021). Although the sediment cores in our study were collected from similar water depths (720-970 m), we observed unsaturated and branched fatty acids, indicating that fatty acid degradation processes, fatty acid sources, or bacterial activity may be different in the Southwestern Ross Sea region compared to Adélie Land. One possible explanation is the markedly higher primary productivity in the Ross Sea, which is considered one of the most productive regions in Antarctica (Bolinesi et al., 2020), with high vertical export of carbon (DeJong et al., 2017), which may lead to enhanced preservation of unsaturated and branched fatty acids in sediments (Ratnarajah et al., 2022; Wakeham et al., 1984). Another possibility is a difference in fatty acid preservation or a difference in fatty acid sources between the southwestern Ross Sea and Adélie Land. Coastal East Antarctica tends to be dominated by diatoms (Heidemann et al., 2024). *P. antarctica* blooms in McMurdo Sound form large colonies (Mangoni et al., 2019; Mangoni et al., 2017), and may contribute to an early and rapid export of carbon to the ocean floor, also leading to enhanced preservation (DiTullio et al., 2000). Another possibility is that the increased abundance of branched and unsaturated fatty acids in the southwestern Ross Sea is related to its lower sedimentation rate (0.225-0.255 cm yr⁻¹) compared with Adélie Land (~1 cm yr⁻¹) (Ashley et al., 2021). Slower sedimentation rates may allow microbial activity to penetrate deeper into the sediment column, promoting greater degradation and alteration of organic matter (Bhattacharya et al., 2021), which may enhance the production or preservation of these fatty acids at depth. The detection of unsaturated and branched fatty acids is consistent with another southwestern Ross Sea (Smith et al., 1986), where a range of unsaturated fatty acids were detected, including PUFAs, which were not identified in our study, but the study was limited to surface sediments.

Degradation can also explain the downcore decline in IPSO₂₅ diene concentrations with sediment depth. IPSO₂₅ shows some decay in the first 10 cm. However, trends in sea ice are preserved as demonstrated by the similar downcore trends seen in the sea ice associated diatoms *F. curta* group and PIPSO₂₅. Sterols did not show a pronounced downcore decay, consistent with their low reactivity (Rontani et al., 2012; Rontani et al., 2019; Vorrath et al., 2019). While IPSO₂₅ shows measurable decay,



the relative reactivity differences between this HBI and the major sterols, brassicasterol and dinosterol, are yet to be quantified. Despite this, PIPSO₂₅ ratios provide representative records of past sea ice extent and climatic conditions, as shown by the Southern Ocean studies linking HBI/sterols with satellite records of sea ice extent (Lamping et al., 2021; Vorrath et al., 2019; Vorrath et al., 2020), diatom transfer functions (Lamping et al., 2020), and ice core records (Vorrath et al., 2023).

4.2 200-year baseline record of sea ice and phytoplankton changes in the southwestern Ross Sea

Downcore records of the *F. curta* group and highly branched isoprenoids (HBIs) were used to examine sea ice variability in the southwestern Ross Sea. The relative abundance *F. curta* decreases downcore in BC02 and BC04, while BC03 shows an increasing trend (Figure 8). Similarly, both IPSO₂₅ diene and PIPSO₂₅, show a decreasing trend downcore. *F. curta* is a well-established sea ice diatom proxy (Gersonde & Zielinski, 2000; Leventer & Dunbar, 1988), particularly associated with seasonal ice zones (Armand et al., 2005), and its presence provides an independent line of evidence to support biomarker-based reconstructions (Gersonde & Zielinski, 2000; Leventer & Dunbar, 1988). Here, the *F. curta* group suggests an overall increase in sea ice activity in the southwestern Ross Sea between 1900 CE to present. from 1900 to present. IPSO₂₅ trends indicate an increased signal of sympagic diatom input and, by extension, greater sea ice presence or duration. The PIPSO₂₅ index integrates IPSO₂₅ diene with open-water sterols, dinosterol and brassicasterol, and is considered a more robust measure of sea ice influence than IPSO₂₅ diene alone (Lamping et al., 2021; Vorrath et al., 2023; Vorrath et al., 2020). Despite the low resolution, the PIPSO₂₅ values in all three cores show an increasing trend since ~1900 CE (Figure 8). Evidence from diatom and biomarker records suggests a 200-year increase in sea ice duration in the southwestern Ross Sea.

Our findings align closely with other Ross Sea records indicating increasing sea ice conditions over the past two centuries. Diatom-based sediment records from the southwestern Ross Sea show a similar long term trend in sea ice presence (Leventer & Dunbar, 1988; Leventer et al., 1993). Yang et al. (2021) reconstructed the northern limit of sea ice extent off the Ross Sea and observed relatively stable conditions pre-1900, followed by an increasing trend since ~1950 CE (Figure 8). Similarly, Dalaiden et al. (2021) used ice core records and data assimilation to reconstruct Ross Sea sea ice extent, also finding an increase beginning around 1950 after a stable pre-1900 period (Figure 8). A coastal ice core record from the Ross Sea shows a stable sea ice area from the 1880s to the 1950s, a reduction from the 1950s to the 1990s and an increase from 1993 (Sinclair et al., 2014). Although these studies quantify sea ice extent and area at the regional scale, and our records reflect coastal sea ice duration at three coastal-proximal sites, most reconstructions point toward enhanced sea ice conditions in the Ross Sea since the mid-20th century (Figure 8).

Differences among studies likely reflect a combination of factors. First, sediment cores generally have lower temporal resolution than ice cores and may not capture short term variations, such as the stable conditions before 1950 reported by Dalaiden et al. (2021) and Yang et al. (2021). Chronological uncertainty is another factor, as the CFCS lead dating model assumes constant sedimentation rates, a constant Pb flux, and no mixing or diffusion of Pb in the sediment (Appleby, 2001; Bruel & Sabatier, 2020). The dating uncertainty could introduce offsets in the timing of the observed trends. Second, spatial variability across the Ross Sea is well documented, with satellite observations from 1997 to 2013 showing an overall increase



in sea ice extent (Yuan et al., 2017), but with significant anomalies across the Ross Sea (Dale et al., 2016; Krauzig et al., 2024). It is plausible that the southwestern Ross Sea experienced an earlier or stronger increase in sea ice duration compared with more northern or offshore regions. Finally, methodological and spatial differences may also contribute. Our records capture
495 sea ice duration and cover near the coast (Armand et al., 2005), while Dalaiden et al. (2021) and Yang et al. (2021) reconstructed sea ice extent at the regional scale. Despite these differences in metric and spatial coverage all records presented in Figure 8 show broadly consistent increases in sea ice conditions since ~1950, underscoring the robustness of this trend across multiple archives and proxies.

Fatty acids in the surface sediments reflect inputs from a mixture of phytoplankton sources, including diatoms and *P.*
500 *antarctica*. However, degradation occurs to ~20 cm depth in downcore records which corresponds with ~76-95 years. After this degradation fatty acid concentrations remain relatively stable. This suggests that early post-depositional alteration is the main control on concentration changes rather than shifts in primary production sources. Beyond the degradation zone, no consistent downcore trends are observed, indicating little change in phytoplankton community composition over the past ~200 years, despite increasing sea-ice influence. However, interpretation is limited by the low sampling resolution (4–8 cm), which
505 may obscure finer-scale variability. Higher-resolution records would allow more detailed reconstruction of short-term variability and potential responses of phytoplankton communities to sea-ice changes.

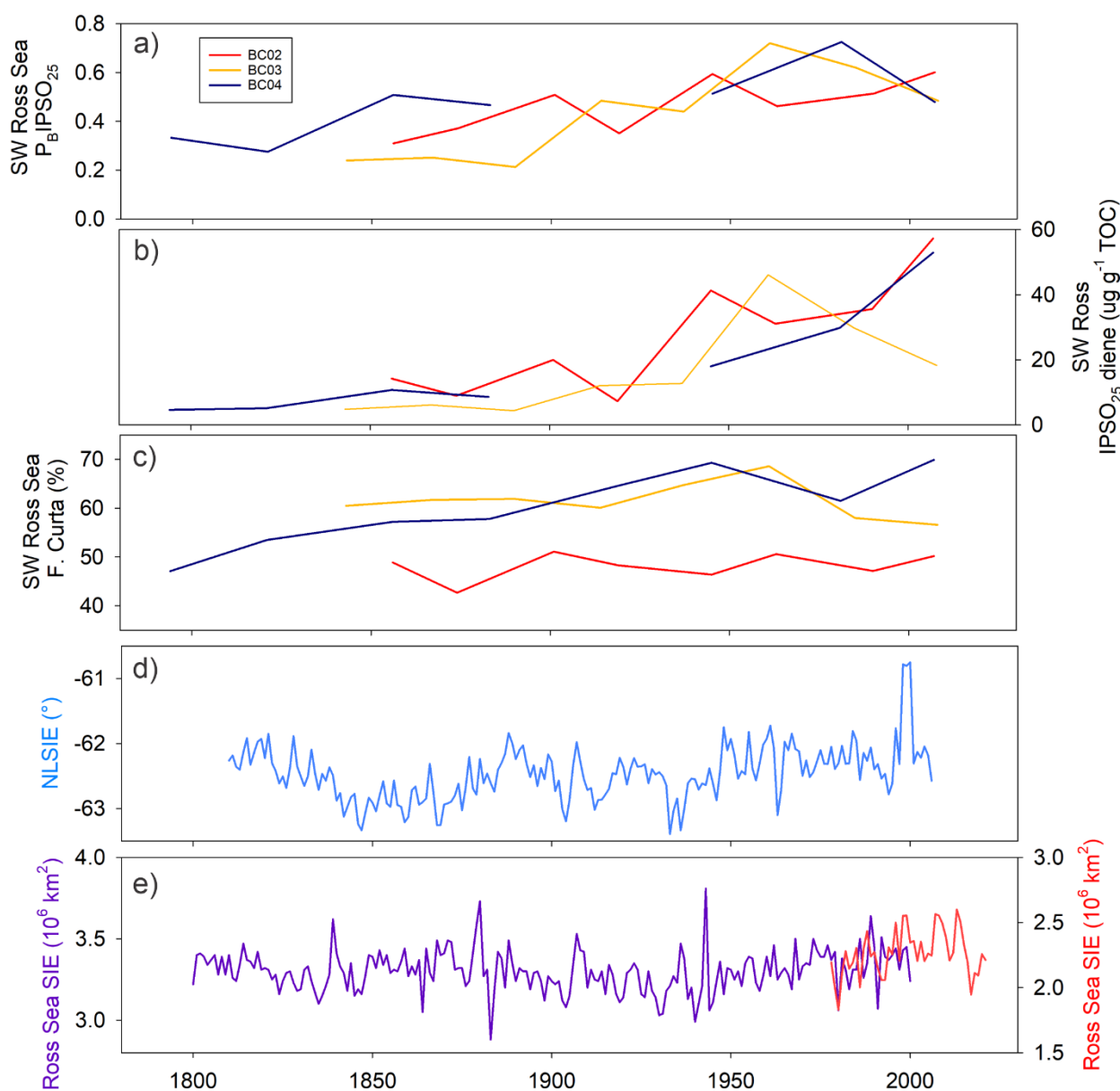


Figure 8: Southwestern Ross Sea sediment results in BC02, BC03, and BC04, a) P_bIPSO_{25} , b) $IPSO_{25}$ diene, c) *Fragilariopsis curta* (*F. curta*). Ross Sea sea ice reconstructions, d) northernmost latitude of sea ice extent in the Ross Sea (NLSIE) (blue) (Yang et al., 2021), e) Ross Sea sea ice extent (SIE) reconstructed using high-resolution ice cores and data assimilation (black) (Dalaiden et al., 2021) and Ross Sea sea ice extent from US National Snow and Ice Data Center (NSIDC) satellite data (red).

510



5 Conclusion

In this study, lipid biomarkers (fatty acids, sterols, and HBIs) from surface and short sediment cores were combined with diatom assemblage data to assess their drivers and help interpret past sea ice dynamics and phytoplankton community changes in a 200-year record in the southwestern Ross Sea. Three sediment cores along a north-south transect were sampled at decadal resolution and dated using ^{210}Pb dating, with the longest core representing years 1794–2007 with an error of ± 20 years at its base. Spatial variations in biomarker composition were primarily driven by sea ice conditions and associated phytoplankton habitats, with pelagic diatoms, *Phaeocystis antarctica*, and sea ice diatoms each exhibiting distinct biomarker signatures. While, pelagic diatom derived fatty acids ($\text{C}_{14:0}$, $\text{C}_{16:0}$, $\text{C}_{16:1\omega 8}$, $\text{C}_{16:1\omega 7}$, $\text{C}_{16:1\omega 6}$, $\text{C}_{16:1\omega 5}$) were identified in this study, polyunsaturated fatty acids (specifically, $\text{C}_{16:4\omega 1}$, $\text{C}_{20:5\omega 3}$, $\text{C}_{20:4\omega 6}$), produced by diatoms, were not detected despite sediments containing abundant preserved diatoms and HBI markers, likely due to grazing, scavenging, and degradation in surface waters and throughout the water column. *Phaeocystis antarctica* fossils are not preserved in marine sediments. However, this study shows that phytoplankton derived fatty acids (high $\text{C}_{14:0}$, $\text{C}_{18:0}$, and $\text{C}_{18:1\omega 9}$, low levels of polyunsaturated fatty acids, and a low $\text{C}_{16:1\omega 7}/\text{C}_{16:0}$ ratio) demonstrate potential to record *Phaeocystis antarctica* variability through time. $\text{C}_{18:0}$ and $\text{C}_{18:1\omega 9}$ decreased along the north to south gradient, which may reflect a difference in phytoplankton community, and/or differing preservation conditions. Biomarkers are also influenced by downcore degradation. Fatty acids in the southwestern Ross Sea demonstrate an overall exponential decay in the top ~ 20 cm of the sediment due to degradation from bacterial biogenesis (demonstrated by 10–20 % of branched fatty acids sourced from bacteria), while still recording the relative composition of phytoplankton groups over this period. Trends in sea ice diatoms such as *Fragilariopsis curta*, and sea ice diatom markers of HBIs, and PIPSO₂₅, reveal a 200-year trend toward increased sea ice extent in the southwestern Ross Sea, aligning with existing regional sea ice extent reconstructions from sediment cores and reconstruction from ice cores which show stability from 1900–1950 but an increase in sea ice to the present. Overall, biomarkers in the southwestern Ross Sea sediment independently distinguish between pelagic diatoms, *Phaeocystis antarctica*, and sea ice associated diatoms, offering a valuable tool for developing decadal resolution records of sea ice and phytoplankton changes in the Ross Sea over the last 2000 years and beyond.

535 Data availability

The data sets for the sediment core age-depth model, organic compound concentrations, diatom abundance, and organic carbon have been submitted to PANGEA data centre. They are included as supplementary material for the purposes of this review.

Author contributions

Conceptualisation: VHLW. Validation: EdJ and SN. Data curation: EdJ. Formal analysis EdJ, SN and VHLW. Investigation: XC, EdJ, SN, VHLW. Methodology: XC, EdJ, SN, and VHLW. Resources: XC, JL, SN, JE and VHLW. Supervision BD, SN



and VHLW. Writing (original draft preparation, review and editing): EdJ. Writing (review and editing): all authors. Funding acquisition; EdJ and VHLW. All authors have read and agreed to the published version of the manuscript.

Competing Interests

Author SN is a member of the editorial board of journal Biogeosciences.

545 Acknowledgements

EM de Jong acknowledges support from Professor James Kennett for supporting the Roger Cooper Masters scholarship in Paleobiology, the Antarctic Research Centre's Endowed Development Fund, and the Trans-Antarctic Association Science Bursary. B Duncan was supported by the New Zealand Ministry of Business Innovation and Employment through the Antarctic Science Platform (ANTA1801). Thank you to A King for helpful feedback on this research and to Sabine Schmidt for advice
550 regarding ^{210}Pb dating. Thank you to KOPRI project PE25090 funded by the Ministry of Oceans and Fisheries for access to core samples.

Financial support

This project was funded by a Rutherford Discovery Fellowship awarded by the Royal Society Te Apārangi (RDF-VUW2203 to VHL Winton) and the Marsden Fund Council from New Zealand Government funding, managed by Royal Society Te
555 Apārangi (MFP-VUW2107 to VHL Winton), and the GNS Science Global Change Through Time program (Strategic Science Investment Fund, Contract ID - C05X1702).



References

- Al-Handal, A. Y., & Wulff, A. (2008). Marine benthic diatoms from Potter Cove, King George Island, Antarctica. <https://doi.org/10.1515/BOT.2008.007>
- Almandoz, G. O., Ferreyra, G. A., Schloss, I. R., Dogliotti, A. I., Rupolo, V., Paparazzo, F. E., Esteves, J. L., & Ferrario, M. E. (2008). Distribution and ecology of *Pseudo-nitzschia* species (Bacillariophyceae) in surface waters of the Weddell Sea (Antarctica). *Polar Biology*, 31(4), 429–442. <https://doi.org/10.1007/s00300-007-0369-9>
- Andreoli, C., Tolomio, C., Moro, I., Radice, M., Moschin, E., & Bellato, S. (1995). Diatoms and dinoflagellates in Terra Nova Bay (Ross Sea-Antarctica) during austral summer 1990. *Polar Biology*, 15(7), 465–475. <https://doi.org/10.1007/BF00237460>
- Appleby, P. (2001). Chronostratigraphic techniques in recent sediments. *Tracking environmental change using lake sediments: basin analysis, coring, and chronological techniques*, 171–203.
- Armand, L. K., Crosta, X., Romero, O., & Pichon, J.-J. (2005). The biogeography of major diatom taxa in Southern Ocean sediments: 1. Sea ice related species. *Palaeogeography, Palaeoclimatology, Palaeoecology*, 223(1–2), 93–126. <https://doi.org/10.1016/j.palaeo.2005.02.015>
- Arrigo, K. R. (2003). A coupled ocean-ecosystem model of the Ross Sea: 2. Iron regulation of phytoplankton taxonomic variability and primary production. *Journal of Geophysical Research*, 108(C7). <https://doi.org/10.1029/2001jc000856>
- Arrigo, K. R., DiTullio, G. R., Dunbar, R. B., Robinson, D. H., VanWoert, M., Worthen, D. L., & Lizotte, M. P. (2000). Phytoplankton taxonomic variability in nutrient utilization and primary production in the Ross Sea. *Journal of Geophysical Research: Oceans*, 105(C4), 8827–8846. <https://doi.org/10.1029/1998JC000289>
- Arrigo, K. R., & van Dijken, G. L. (2004). Annual changes in sea-ice, chlorophyll a, and primary production in the Ross Sea, Antarctica. *Deep Sea Research Part II: Topical Studies in Oceanography*, 51(1–3), 117–138. <https://doi.org/10.1016/j.dsr2.2003.04.003>
- Arrigo, K. R., van Dijken, G. L., & Strong, A. L. (2015). Environmental controls of marine productivity hot spots around Antarctica. *Journal of Geophysical Research: Oceans*, 120(8), 5545–5565. <https://doi.org/10.1002/2015jc010888>
- Ashley, K. E., Crosta, X., Etourneau, J., Campagne, P., Gilchrist, H., Ibraheem, U., Greene, S. E., Schmidt, S., Eley, Y., Massé, G., & Bendle, J. (2021). Exploring the use of compound-specific carbon isotopes as a palaeoproductivity proxy off the coast of Adélie Land, East Antarctica. *Biogeosciences*, 18(19), 5555–5571. <https://doi.org/10.5194/bg-18-5555-2021>
- Baldauf, J. G., & Barron, J. A. (1991). 29. DIATOM BIOSTRATIGRAPHY: KERGUELEN PLATEAU AND PRYDZ BAY REGIONS OF THE SOUTHERN OCEAN. 1. Barron, J., Larsen, B. et al,
- Barbara, L., Crosta, X., Leventer, A., Schmidt, S., Etourneau, J., Domack, E., & Massé, G. (2016). Environmental responses of the Northeast Antarctic Peninsula to the Holocene climate variability. *Paleoceanography*, 31(1), 131–147. <https://doi.org/10.1002/2015PA002785>
- Belt, S. T. (2018). Source-specific biomarkers as proxies for Arctic and Antarctic sea ice. *Organic Geochemistry*, 125, 277–298. <https://doi.org/10.1016/j.orggeochem.2018.10.002>
- Belt, S. T., & Müller, J. (2013). The Arctic sea ice biomarker IP25: a review of current understanding, recommendations for future research and applications in palaeo sea ice reconstructions. *Quaternary Science Reviews*, 79, 9–25. <https://doi.org/10.1016/j.quascirev.2012.12.001>
- Belt, S. T., Smik, L., Brown, T. A., Kim, J.-H., Rowland, S., Allen, C. S., Gal, J.-K., Shin, K.-H., Lee, J. I., & Taylor, K. (2016). Source identification and distribution reveals the potential of the geochemical Antarctic sea ice proxy IPSO25. *Nature communications*, 7(1), 12655. <https://doi.org/10.1038/ncomms12655>
- Bhattacharya, S., Mapder, T., Fernandes, S., Roy, C., Sarkar, J., Rameez, M. J., Mandal, S., Sar, A., Chakraborty, A. K., & Mondal, N. (2021). Sedimentation rate and organic matter dynamics shape microbiomes across a continental margin. *Biogeosciences Discussions*, 2021, 1–39. <https://doi.org/10.5194/bg-18-5203-2021>
- Bolinesi, F., Saggiomo, M., Ardini, F., Castagno, P., Cordone, A., Fusco, G., Rivaro, P., Saggiomo, V., & Mangoni, O. (2020). Spatial-Related Community Structure and Dynamics in Phytoplankton of the Ross Sea, Antarctica. *Frontiers in Marine Science*, 7. <https://doi.org/10.3389/fmars.2020.574963>
- Boyd, P. W., Lennartz, S. T., Glover, D. M., & Doney, S. C. (2015). Biological ramifications of climate-change-mediated oceanic multi-stressors. *Nature Climate Change*, 5(1), 71–79. <https://doi.org/10.1038/NCLIMATE2441>
- Brett, G., Irvin, A., Rack, W., Haas, C., Langhorne, P., & Leonard, G. (2020). Variability in the distribution of fast ice and the sub-ice platelet layer near McMurdo Ice Shelf. *Journal of Geophysical Research: Oceans*, 125(3), e2019JC015678. <https://doi.org/10.1029/2019JC015678>
- Bruel, R., & Sabatier, P. (2020). serac: an R package for ShortlivEd RAdionuclide chronology of recent sediment cores. *J Environ Radioact*, 225, 106449. <https://doi.org/10.1016/j.jenvrad.2020.106449>
- Burckle, L. H. (1984). Diatom distribution and paleoceanographic reconstruction in the Southern Ocean—Present and Last Glacial Maximum. *Marine Micropaleontology*, 9(3), 241–261. [https://doi.org/10.1016/0377-8398\(84\)90015-X](https://doi.org/10.1016/0377-8398(84)90015-X)



- Cau, A., Ennas, C., Moccia, D., Mangoni, O., Bolinesi, F., Saggiomo, M., Granata, A., Guglielmo, L., Swadling, K. M., & Pusceddu, A. (2021). Particulate organic matter release below melting sea ice (Terra Nova Bay, Ross Sea, Antarctica): Possible relationships with zooplankton. *Journal of marine Systems*, 217. <https://doi.org/10.1016/j.jmarsys.2021.103510>
- 615 Crosta, X., & Koç, N. (2007). Chapter eight diatoms: From micropaleontology to isotope geochemistry. *Developments in marine geology*, 1, 327-369. [https://doi.org/10.1016/S1572-5480\(07\)01013-5](https://doi.org/10.1016/S1572-5480(07)01013-5)
- Crosta, X., Romero, O., Armand, L. K., & Pichon, J.-J. (2005). The biogeography of major diatom taxa in Southern Ocean sediments: 2. Open ocean related species. *Palaeogeography, Palaeoclimatology, Palaeoecology*, 223(1-2), 66-92.
- Crosta, X., Shukla, S. K., Ther, O., Ikehara, M., Yamane, M., & Yokoyama, Y. (2020). Last Abundant Appearance Datum of Hemidiscus karstenii driven by climate change. *Marine Micropaleontology*, 157, 101861. <https://doi.org/10.1016/j.marmicro.2020.101861>
- 620 Crosta, X., Sturm, A., Armand, L., & Pichon, J.-J. (2004). Late Quaternary sea ice history in the Indian sector of the Southern Ocean as recorded by diatom assemblages. *Marine Micropaleontology*, 50(3-4), 209-223. [https://doi.org/10.1016/S0377-8398\(03\)00072-0](https://doi.org/10.1016/S0377-8398(03)00072-0)
- Cunningham, W. L., & Leventer, A. (1998). Diatom assemblages in surface sediments of the Ross Sea: relationship to present oceanographic conditions. *Antarctic Science*, 10(2), 134-146. <https://doi.org/10.1017/S0954102098000182>
- 625 Cunningham, W. L., Leventer, A., Andrews, J. T., Jennings, A. E., & Licht, K. J. (1999). Late Pleistocene-Holocene marine conditions in the Ross Sea, Antarctica: evidence from the diatom record. *The Holocene*, 9(2), 129-139. <https://doi.org/10.1191/095968399675624796>
- Dalaiden, Q., Goosse, H., Rezsöházy, J., & Thomas, E. R. (2021). Reconstructing atmospheric circulation and sea-ice extent in the West Antarctic over the past 200 years using data assimilation. *Climate Dynamics*, 57(11), 3479-3503. <https://doi.org/10.1007/s00382-021-05879-6>
- 630 Dale, E. R., McDonald, A. J., Coggins, J. H., & Rack, W. (2016). Atmospheric forcing of sea ice anomalies in the Ross Sea polynya region. *The Cryosphere Discussions*, 2016, 1-21. <https://doi.org/10.5194/tc-11-267-2017>
- DeJong, H. B., Dunbar, R. B., Kowek, D. A., Mucciarone, D. A., Bercovici, S. K., & Hansell, D. A. (2017). Net community production and carbon export during the late summer in the Ross Sea, Antarctica. *Global Biogeochemical Cycles*, 31(3), 473-491. <https://doi.org/10.1002/2016GB005417>
- 635 Deppeler, S. L., & Davidson, A. T. (2017). Southern Ocean Phytoplankton in a Changing Climate. *Frontiers in Marine Science*, 4. <https://doi.org/10.3389/fmars.2017.00040>
- DiTullio, G., Grebmeier, J., Arrigo, K., Lizotte, M., Robinson, D., Leventer, A., Barry, J., VanWoert, M., & Dunbar, R. (2000). Rapid and early export of Phaeocystis antarctica blooms in the Ross Sea, Antarctica. *Nature*, 404(6778), 595-598. <https://doi.org/10.1038/35007061>
- 640 Dong, Y., Bakker, D. C., Bell, T. G., Yang, M., Landschützer, P., Hauck, J., Rödenbeck, C., Kitidis, V., Bushinsky, S. M., & Liss, P. S. (2024). Direct observational evidence of strong CO₂ uptake in the Southern Ocean. *Science Advances*, 10(30), eadn5781. <https://doi.org/10.1126/sciadv.adn5781>
- Eikrem, W., Medlin, L. K., Henderiks, J., Rokitta, S., Rost, B., Probert, I., Throndsen, J., & Edvardsen, B. (2016). Haptophyta. In *Handbook of the Protists* (pp. 1-61). Springer. https://doi.org/10.1007/978-3-319-32669-6_38-1
- 645 Elliott, D. T., Tang, K. W., & Shields, A. R. (2009). Mesozooplankton beneath the summer sea ice in McMurdo Sound, Antarctica: abundance, species composition, and DMSP content. *Polar Biology*, 32, 113-122. <https://doi.org/10.1007/s00300-008-0511-3>
- Etourneau, J., Collins, L. G., Willmott, V., Kim, J. H., Barbara, L., Leventer, A., Schouten, S., Sinninghe Damsté, J. S., Bianchini, A., Klein, V., Crosta, X., & Massé, G. (2013). Holocene climate variations in the western Antarctic Peninsula: evidence for sea ice extent predominantly controlled by changes in insolation and ENSO variability. *Climate of the Past*, 9(4), 1431-1446. <https://doi.org/10.5194/cp-9-1431-2013>
- 650 Fahl, K., & Kattner, G. (1993). Lipid content and fatty acid composition of algal communities in sea-ice and water from the Weddell Sea (Antarctica). *Polar Biology*, 13, 405-409. <https://doi.org/10.1007/BF01681982>
- Gersonde, R., & Zielinski, U. (2000). The reconstruction of late Quaternary Antarctic sea-ice distribution—the use of diatoms as a proxy for sea-ice. *Palaeogeography, Palaeoclimatology, Palaeoecology*, 162(3-4), 263-286. [https://doi.org/10.1016/S0031-0182\(00\)00131-0](https://doi.org/10.1016/S0031-0182(00)00131-0)
- 655 Guo, X., Zhao, J., Pan, J., & Sun, Y. (2024). Organic matter composition in sediments recording sea surface phytoplankton community structure in Prydz Bay of Antarctica. *Organic Geochemistry*, 104828. <https://doi.org/10.1016/j.orggeochem.2024.104828>
- Haddad, R. I., Martens, C. S., & Farrington, J. W. (1992). Quantifying early diagenesis of fatty acids in a rapidly accumulating coastal marine sediment. *Organic Geochemistry*, 19(1-3), 205-216. [https://doi.org/10.1016/0146-6380\(92\)90037-X](https://doi.org/10.1016/0146-6380(92)90037-X)
- 660 Hamm, C., Reigstad, M., Riser, C. W., Mühlebach, A., & Wassmann, P. (2001). On the trophic fate of Phaeocystis pouchetii. VII. Sterols and fatty acids reveal sedimentation of P. pouchetii-derived organic matter via krill fecal strings. *Marine Ecology progress series*, 209, 55-69. <https://doi.org/10.3354/meps209055>
- Hayward, A., Pinkerton, M. H., & Gutierrez-Rodriguez, A. (2023). phytoclass: A pigment-based chemotaxonomic method to determine the biomass of phytoplankton classes. *Limnology and Oceanography: Methods*, 21(4), 220-241. <https://doi.org/10.1002/lom3.10541>



- 665 Hayward, A., Wright, S. W., Carroll, D., Law, C. S., Wongpan, P., Gutiérrez-Rodríguez, A., & Pinkerton, M. H. (2025). Antarctic phytoplankton communities restructure under shifting sea-ice regimes. *Nature Climate Change*, 1-8. <https://doi.org/10.1038/s41558-025-02379-x>
- Heidemann, A. C., Westwood, K. J., Foppert, A., Wright, S. W., Klocker, A., Vives, C. R., Wotherspoon, S., & Bestley, S. (2024). Drivers of phytoplankton distribution, abundance and community composition off East Antarctica, from 55-80° E (CCAMLR Division 58.4. 2 East). *Frontiers in Marine Science*, 11, 1454421. <https://doi.org/10.3389/fmars.2024.1454421>
- 670 Henley, S. F., Cavan, E. L., Fawcett, S. E., Kerr, R., Monteiro, T., Sherrell, R. M., Bowie, A. R., Boyd, P. W., Barnes, D. K. A., Schloss, I. R., Marshall, T., Flynn, R., & Smith, S. (2020). Changing Biogeochemistry of the Southern Ocean and Its Ecosystem Implications. *Frontiers in Marine Science*, 7. <https://doi.org/10.3389/fmars.2020.00581>
- Johns, L., Wraige, E., Belt, S., Lewis, C., Massé, G., Robert, J.-M., & Rowland, S. (1999). Identification of a C25 highly branched isoprenoid (HBI) diene in Antarctic sediments, Antarctic sea-ice diatoms and cultured diatoms. *Organic Geochemistry*, 30(11), 1471-1475. [https://doi.org/10.1016/S0146-6380\(99\)00112-6](https://doi.org/10.1016/S0146-6380(99)00112-6)
- 675 Johnson, K. M., McKay, R. M., Etourneau, J., Jiménez-Espejo, F. J., Albot, A., Riesselman, C. R., Bertler, N. A., Horgan, H. J., Crosta, X., & Bendle, J. (2021). Sensitivity of Holocene East Antarctic productivity to subdecadal variability set by sea ice. *Nature Geoscience*, 1-7. <https://doi.org/10.1038/s41561-021-00816-y>
- 680 Kalpana, M., Routh, J., Fietz, S., Lone, M. A., & Mangini, A. (2021). Sources, Distribution and Paleoenvironmental Application of Fatty Acids in Speleothem Deposits From Krem Mawmluh, Northeast India. *Frontiers in Earth Science*, 9, 687376. <https://doi.org/10.3389/feart.2021.687376>
- Kaneda, T. (1991). Iso-and anteiso-fatty acids in bacteria: biosynthesis, function, and taxonomic significance. *Microbiological reviews*, 55(2), 288-302. <https://doi.org/10.1128/mr.55.2.288-302.1991>
- 685 Krauzig, N., Flocco, D., Kern, S., & Zambianchi, E. (2024). Exploring sea ice transport dynamics at the eastern gate of the Ross Sea. *Deep Sea Research Part II: Topical Studies in Oceanography*, 218, 105428. <https://doi.org/10.1016/j.dsr2.2024.105428>
- Lamping, N., Müller, J., Esper, O., Hillenbrand, C.-D., Smith, J. A., & Kuhn, G. (2020). Highly branched isoprenoids reveal onset of deglaciation followed by dynamic sea-ice conditions in the western Amundsen Sea, Antarctica. *Quaternary Science Reviews*, 228, 106103. <https://doi.org/10.1016/j.quascirev.2019.106103>
- 690 Lamping, N., Müller, J., Heftner, J., Mollenhauer, G., Haas, C., Shi, X., Vorrath, M.-E., Lohmann, G., & Hillenbrand, C.-D. (2021). Evaluation of lipid biomarkers as proxies for sea ice and ocean temperatures along the Antarctic continental margin. *Climate of the Past*, 17(5), 2305-2326. <https://doi.org/10.5194/cp-17-2305-2021>
- Leventer, A., & Dunbar, R. B. (1988). Recent diatom record of McMurdo Sound, Antarctica: Implications for history of sea ice extent. *Paleoceanography*, 3(3), 259-274. <https://doi.org/10.1029/PA003i003p00259>
- 695 Leventer, A., Dunbar, R. B., & DeMaster, D. J. (1993). Diatom evidence for late Holocene climatic events in Granite Harbor, Antarctica. *Paleoceanography*, 8(3), 373-386. <https://doi.org/10.1029/93PA00561>
- Mangoni, O., Saggiomo, M., Bolinesi, F., Castellano, M., Povero, P., Saggiomo, V., & DiTullio, G. R. (2019). Phaeocystis antarctica unusual summer bloom in stratified antarctic coastal waters (Terra Nova Bay, Ross Sea). *Marine environmental research*, 151, 104733. <https://doi.org/10.1016/j.marenvres.2019.05.012>
- 700 Mangoni, O., Saggiomo, V., Bolinesi, F., Margiotta, F., Budillon, G., Cotroneo, Y., Misic, C., Rivaro, P., & Saggiomo, M. (2017). Phytoplankton blooms during austral summer in the Ross Sea, Antarctica: Driving factors and trophic implications. *PLoS One*, 12(4), e0176033. <https://doi.org/10.1371/journal.pone.0176033>
- Matsuoka, K., Skoglund, A., Roth, G., de Pomereu, J., Griffiths, H., Headland, R., Herried, B., Katsumata, K., Le Brocq, A., Licht, K., Morgan, F., Neff, P. D., Ritz, C., Scheinert, M., Tamura, T., Van de Putte, A., van den Broeke, M., von Deschwandén, A., Deschamps-Berger, C., Van Liefferinge, B., Tronstad, S., & Melvær, Y. (2021). Quantarctica, an integrated mapping environment for Antarctica, the Southern Ocean, and sub-Antarctic islands. *Environmental Modelling & Software*, 140. <https://doi.org/10.1016/j.envsoft.2021.105015>
- 705 McMinn, A., Martin, A., & Ryan, K. (2010). Phytoplankton and sea ice algal biomass and physiology during the transition between winter and spring (McMurdo Sound, Antarctica). *Polar Biology*, 33, 1547-1556. <https://doi.org/10.1007/s00300-010-0844-6>
- 710 Meyers, P. A. (1997). Organic geochemical proxies of paleoceanographic, paleolimnologic, and paleoclimatic processes. *Organic Geochemistry*, 27(5-6), 213-250. [https://doi.org/10.1016/S0146-6380\(97\)00049-1](https://doi.org/10.1016/S0146-6380(97)00049-1)
- Mezgec, K., Stenni, B., Crosta, X., Masson-Delmotte, V., Baroni, C., Braidà, M., Ciardini, V., Colizza, E., Melis, R., Salvatore, M. C., Severi, M., Scarchilli, C., Traversi, R., Udisti, R., & Frezzotti, M. (2017). Holocene sea ice variability driven by wind and polynya efficiency in the Ross Sea. *Nat Commun*, 8(1), 1334. <https://doi.org/10.1038/s41467-017-01455-x>
- 715 Moriwaki, K. (1990). Diatoms in water column and sea-ice in Lützow-Holm Bay, Antarctica, and their preservation in the underlying sediments. *Bulletin of the National Science Museum. Series C*, 16(1), 15-39.
- Nacher, S., Smittenberg, R. H., Gilli, A., Kirilova, E. P., Lotter, A. F., & Schubert, C. J. (2012). Impact of recent lake eutrophication on microbial community changes as revealed by high resolution lipid biomarkers in Rotsee (Switzerland). *Organic Geochemistry*, 49, 86-95. <https://doi.org/10.1016/j.orggeochem.2012.05.014>



- 720 Nichols, D. S., Nichols, P. D., & Sullivan, C. W. (1993). Fatty acid, sterol and hydrocarbon composition of Antarctic sea ice diatom communities during the spring bloom in McMurdo Sound. *Antarctic Science*, 5(3), 271-278. <https://doi.org/10.1017/S0954102093000367>
- Nichols, P. D., Palmisano, A. C., Smith, G. A., & White, D. C. (1986). Lipids of the Antarctic sea ice diatom *Nitzschia cylindrus*. *Phytochemistry*, 25(7), 1649-1653. [https://doi.org/10.1016/S0031-9422\(00\)81228-5](https://doi.org/10.1016/S0031-9422(00)81228-5)
- 725 Nichols, P. D., Skerratt, J. H., Davidson, A., Burton, H., & McMeekin, T. A. (1991). Lipids of cultured *Phaeocystis pouchetii*: signatures for food-web, biogeochemical and environmental studies in Antarctica and the Southern Ocean. *Phytochemistry*, 30(10), 3209-3214. [https://doi.org/10.1016/0031-9422\(91\)83177-M](https://doi.org/10.1016/0031-9422(91)83177-M)
- Noble, A. E., Moran, D. M., Allen, A. E., & Saito, M. A. (2013). Dissolved and particulate trace metal micronutrients under the McMurdo Sound seasonal sea ice: basal sea ice communities as a capacitor for iron. *Frontiers in Chemistry*, 1, 25. <https://doi.org/10.3389/fchem.2013.00025>
- 730 Peck, V. L., Allen, C. S., Kender, S., McClymont, E. L., & Hodgson, D. A. (2015). Oceanographic variability on the West Antarctic Peninsula during the Holocene and the influence of upper circumpolar deep water. *Quaternary Science Reviews*, 119, 54-65. <https://doi.org/10.1016/j.quascirev.2015.04.002>
- Pinkerton, M. H., Boyd, P. W., Deppeler, S., Hayward, A., Höfer, J., & Moreau, S. (2021). Evidence for the impact of climate change on primary producers in the Southern Ocean. *Frontiers in Ecology and Evolution*, 9, 134. <https://doi.org/10.3389/fevo.2021.592027>
- 735 Rampen, S. W., Abbas, B. A., Schouten, S., & Sinninghe Damste, J. S. (2010). A comprehensive study of sterols in marine diatoms (Bacillariophyta): Implications for their use as tracers for diatom productivity. *Limnology and oceanography*, 55(1), 91-105. <https://doi.org/10.4319/lo.2010.55.1.0091>
- Ratnarajah, L., Puigcorb , V., Moreau, S., Roca-Mart , M., Janssens, J., Corkill, M., Duprat, L., Genovese, C., Lieser, J., & Masqu , P. (2022). Distribution and export of particulate organic carbon in East Antarctic coastal polynyas. *Deep Sea Research Part I: Oceanographic Research Papers*, 190, 103899. <https://doi.org/10.1016/j.dsr.2022.103899>
- Riaux-Gobin, C., Poulin, M., Dieckmann, G., Labrun , C., & V tion, G. (2011). Spring phytoplankton onset after the ice break-up and sea-ice signature (Ad lie Land, East Antarctica). *Polar Research*, 30(1), 5910. <https://doi.org/10.3402/polar.v30i0.5910>
- 745 Rontani, J.-F., Charriere, B., Forest, A., Heussner, S., Vaultier, F., Petit, M., Delsaut, N., Fortier, L., & Sempere, R. (2012). Intense photooxidative degradation of planktonic and bacterial lipids in sinking particles collected with sediment traps across the Canadian Beaufort Shelf (Arctic Ocean). *Biogeosciences*, 9(11), 4787-4802. <https://doi.org/10.5194/bg-9-4787-2012>
- Rontani, J.-F., Smik, L., Belt, S. T., Vaultier, F., Armbr cht, L., Leventer, A., & Armand, L. K. (2019). Abiotic degradation of highly branched isoprenoid alkenes and other lipids in the water column off East Antarctica. *Marine Chemistry*, 210, 34-47. <https://doi.org/10.1016/j.marchem.2019.02.004>
- 750 Ryan-Keogh, T. J., DeLizo, L. M., Smith Jr, W. O., Sedwick, P. N., McGillicuddy Jr, D. J., Moore, C. M., & Bibby, T. S. (2017). Temporal progression of photosynthetic-strategy in phytoplankton in the Ross Sea, Antarctica. *Journal of marine Systems*, 166, 87-96. <https://doi.org/https://doi.org/10.1016/j.jmarsys.2016.08.014>
- Sadatzi, H., Opdyke, B., Menviel, L., Leventer, A., Hope, J. M., Brocks, J. J., Fallon, S., Post, A. L., O'brien, P. E., & Grant, K. (2023). Early sea ice decline off East Antarctica at the last glacial–interglacial climate transition. *Science Advances*, 9(41), eadh9513. <https://doi.org/10.1126/sciadv.adh9513>
- 755 Saggiomo, M., Escalera, L., Bolinesi, F., Rivaro, P., Saggiomo, V., & Mangoni, O. (2021). Diatom diversity during two austral summers in the Ross Sea (Antarctica). *Marine Micropaleontology*, 165. <https://doi.org/10.1016/j.marmicro.2021.101993>
- Schmidt, K., Brown, T. A., Belt, S. T., Ireland, L. C., Taylor, K. W., Thorpe, S. E., Ward, P., & Atkinson, A. (2018). Do pelagic grazers benefit from sea ice? Insights from the Antarctic sea ice proxy IPSO 25. *Biogeosciences*, 15(7), 1987-2006. <https://doi.org/10.5194/bg-15-1987-2018>
- 760 Schofield, O., Cimino, M., Doney, S., Friedlaender, A., Meredith, M., Moffat, C., Stammerjohn, S., Van Mooy, B., & Steinberg, D. (2024). Antarctic pelagic ecosystems on a warming planet. *Trends in ecology & evolution*. <https://doi.org/10.1016/j.tree.2024.08.007> 1
- Sinclair, K. E., Bertler, N. A. N., Bowen, M. M., & Arrigo, K. R. (2014). Twentieth century sea-ice trends in the Ross Sea from a high-resolution, coastal ice-core record. *Geophysical research letters*, 41(10), 3510-3516. <https://doi.org/10.1002/2014gl059821>
- 765 Skerratt, J., Nichols, P., McMeekin, T., & Burton, H. (1995). Seasonal and inter-annual changes in planktonic biomass and community structure in eastern Antarctica using signature lipids. *Marine Chemistry*, 51(2), 93-113. [https://doi.org/10.1016/0304-4203\(95\)00047-U](https://doi.org/10.1016/0304-4203(95)00047-U)
- Skerratt, J. H., Davidson, A. D., Nichols, P. D., & McMeekin, T. A. (1998). Effect of UV-B on lipid content of three Antarctic marine phytoplankton. *Phytochemistry*, 49(4), 999-1007. [https://doi.org/10.1016/S0031-9422\(97\)01068-6](https://doi.org/10.1016/S0031-9422(97)01068-6)
- 770 Smik, L., Belt, S. T., Lieser, J. L., Armand, L. K., & Leventer, A. (2016). Distributions of highly branched isoprenoid alkenes and other algal lipids in surface waters from East Antarctica: Further insights for biomarker-based paleo sea-ice reconstruction. *Organic Geochemistry*, 95, 71-80. <https://doi.org/10.1016/j.orggeochem.2016.02.011>
- Smik, L., Cabedo-Sanz, P., & Belt, S. T. (2016). Semi-quantitative estimates of paleo Arctic sea ice concentration based on source-specific highly branched isoprenoid alkenes: A further development of the PIP25 index. *Organic Geochemistry*, 92, 63-69. <https://doi.org/10.1016/j.orggeochem.2015.12.007>
- 775



- Smith, G. A., Nichols, P. D., & White, D. C. (1986). Fatty acid composition and microbial activity of benthic marine sediment from McMurdo Sound, Antarctica. *FEMS Microbiology Ecology*, 2(4), 219-231. <https://doi.org/10.1111/j.1574-6968.1986.tb01732.x>
- Spreen, G., Kaleschke, L., & Heygster, G. (2008). Sea ice remote sensing using AMSR-E 89-GHz channels. *Journal of Geophysical Research: Oceans*, 113(C2).
- 780 Stoecker, D. K., Putt, M., & Moisan, T. (1995). Nano-and microplankton dynamics during the spring *Phaeocystis* sp. bloom in McMurdo Sound, Antarctica. *Journal of the Marine Biological Association of the United Kingdom*, 75(4), 815-832. <https://doi.org/10.1017/S0025315400038170>
- Tesi, T., Belt, S. T., Gariboldi, K., Muschitiello, F., Smik, L., Finocchiaro, F., Giglio, F., Colizza, E., Gazzurra, G., Giordano, P., Morigi, C., Capotondi, L., Nogarotto, A., Köseoğlu, D., Di Roberto, A., Gallerani, A., & Langone, L. (2020). Resolving sea ice dynamics in the north-western Ross Sea during the last 2.6 ka: From seasonal to millennial timescales. *Quaternary Science Reviews*, 237. <https://doi.org/10.1016/j.quascirev.2020.106299>
- 785 Thomas, E. R., Allen, C. S., Etourneau, J., King, A. C., Severi, M., Winton, V. H. L., Mueller, J., Crosta, X., & Peck, V. L. (2019). Antarctic sea ice proxies from marine and ice core archives suitable for reconstructing sea ice over the past 2000 Years. *Geosciences*, 9(12), 506. <https://doi.org/10.3390/geosciences9120506>
- 790 Thomson, P. G., Wright, S. W., Bolch, C. J., Nichols, P. D., Skerratt, J. H., & McMinn, A. (2004). Antarctic Distribution, Pigment and Lipid Composition, and Molecular Identification of the Brine Dinoflagellate *Polarella glacialis* (DINOPHYCEAE) 1. *Journal of Phycology*, 40(5), 867-873. <https://doi.org/10.1111/j.1529-8817.2004.03169.x>
- Villinski, J. C., Hayes, J. M., Brassell, S. C., Riggert, V. L., & Dunbar, R. B. (2008). Sedimentary sterols as biogeochemical indicators in the Southern Ocean. *Organic Geochemistry*, 39(5), 567-588. <https://doi.org/10.1016/j.orggeochem.2008.01.009>
- 795 Volkman, J. K. (2006). Lipid markers for marine organic matter. *Marine organic matter: Biomarkers, isotopes and DNA*, 27-70. https://doi.org/10.1007/698_2_002
- Vorrath, M.-E., Müller, J., Cárdenas, P., Opel, T., Mieruch, S., Esper, O., Lembke-Jene, L., Etourneau, J., Vieth-Hillebrand, A., & Lahajnar, N. (2023). Deglacial and Holocene sea-ice and climate dynamics in the Bransfield Strait, northern Antarctic Peninsula. *Climate of the Past*, 19(5), 1061-1079. <https://doi.org/10.5194/cp-19-1061-2023>
- 800 Vorrath, M.-E., Müller, J., Esper, O., Mollenhauer, G., Haas, C., Schefuß, E., & Fahl, K. (2019). Highly branched isoprenoids for Southern Ocean sea ice reconstructions: a pilot study from the Western Antarctic Peninsula. *Biogeosciences*, 16(15), 2961-2981. <https://doi.org/10.5194/bg-16-2961-2019>
- Vorrath, M.-E., Müller, J., Rebolledo, L., Cárdenas, P., Shi, X., Esper, O., Opel, T., Geibert, W., Muñoz, P., Haas, C., Kuhn, G., Lange, C. B., Lohmann, G., & Mollenhauer, G. (2020). Sea ice dynamics in the Bransfield Strait, Antarctic Peninsula, during the past 240 years: a multi-proxy intercomparison study. *Climate of the Past*, 16(6), 2459-2483. <https://doi.org/10.5194/cp-16-2459-2020>
- 805 Wakeham, S. G., Farrington, J. W., & Gagosian, R. B. (1984). Variability in lipid flux and composition of particulate matter in the Peru upwelling region. *Organic Geochemistry*, 6, 203-215. [https://doi.org/10.1016/0146-6380\(84\)90042-1](https://doi.org/10.1016/0146-6380(84)90042-1)
- Wakeham, S. G., Hedges, J. I., Lee, C., Peterson, M. L., & Hernes, P. J. (1997). Compositions and transport of lipid biomarkers through the water column and surficial sediments of the equatorial Pacific Ocean. *Deep Sea Research Part II: Topical Studies in Oceanography*, 44(9-10), 2131-2162. [https://doi.org/10.1016/S0967-0645\(97\)00035-0](https://doi.org/10.1016/S0967-0645(97)00035-0)
- 810 Warnock, J. P., & Scherer, R. P. (2015). Diatom species abundance and morphologically-based dissolution proxies in coastal Southern Ocean assemblages. *Continental Shelf Research*, 102, 1-8. <https://doi.org/10.1016/j.csr.2015.04.012>
- Willis, M. D., Lannuzel, D., Else, B., Angot, H., Campbell, K., Crabeck, O., Delille, B., Hayashida, H., Lizotte, M., & Loose, B. (2023). Polar oceans and sea ice in a changing climate. *Elementa*, 11(1). <https://doi.org/10.1525/elementa.2023.00056>
- 815 Wilson, S., Steinberg, D., Chu, F.-L., & Bishop, J. (2010). Feeding ecology of mesopelagic zooplankton of the subtropical and subarctic North Pacific Ocean determined with fatty acid biomarkers. *Deep Sea Research Part I: Oceanographic Research Papers*, 57(10), 1278-1294. <https://doi.org/10.1016/j.dsr.2010.07.005>
- Wing, S., McLeod, R., Leichter, J., Frew, R., & Lamare, M. (2012). Sea ice microbial production supports Ross Sea benthic communities: influence of a small but stable subsidy. *Ecology*, 93(2), 314-323. <https://doi.org/10.1890/11-0996.1>
- 820 Winton, V., Edwards, R., Delmonte, B., Ellis, A., Andersson, P., Bowie, A., Bertler, N., Neff, P., & Tuohy, A. (2016). Multiple sources of soluble atmospheric iron to Antarctic waters. *Global Biogeochemical Cycles*, 30(3), 421-437. <https://doi.org/10.1002/2015GB005265>
- Wisniewski, E., Bicego, M. C., Montone, R. C., Figueira, R. C., Ceschim, L. M., Mahiques, M. M., & Martins, C. C. (2014). Characterization of sources and temporal variation in the organic matter input indicated by n-alkanols and sterols in sediment cores from Admiralty Bay, King George Island, Antarctica. *Polar Biology*, 37, 483-496. <https://doi.org/10.1007/s00300-014-1445-6>
- 825 Yang, G., Li, C., Guilini, K., Peng, Q., Wang, Y., Zhang, Y., & Zhang, Y. (2016). Feeding strategies of four dominant copepod species in Prydz Bay, Antarctica: insights from a combined fatty acid biomarker and stable isotopic approach. *Deep Sea Research Part I: Oceanographic Research Papers*, 114, 55-63. <https://doi.org/10.1016/j.dsr.2016.04.016>
- Yang, J., Xiao, C., Liu, J., Li, S., & Qin, D. (2021). Variability of Antarctic sea ice extent over the past 200 years. *Science Bulletin*, 66(23), 2394-2404. <https://doi.org/10.1016/j.scib.2021.07.028>
- 830



Yuan, N., Ding, M., Ludescher, J., & Bunde, A. (2017). Increase of the Antarctic Sea Ice Extent is highly significant only in the Ross Sea. *Sci Rep*, 7, 41096. <https://doi.org/10.1038/srep41096>